Sedimentary Geology 294 (2013) 219–232

Contents lists available at SciVerse ScienceDirect

Sedimentary Geology

journal homepage: www.elsevier.com/locate/sedgeo

Invited review

Neoproterozoic glaciations in a revised global palaeogeography from the breakup of Rodinia to the assembly of Gondwanaland

Zheng-Xiang Li [a,b,*], David A.D. Evans [b], Galen P. Halverson [c,d]

[a] ARC Centre of Excellence for Core to Crust Fluid Systems (CCFS) and The Institute for Geoscience Research (TIGeR), Department of Applied Geology, Curtin University, GPO Box U1987, Perth, WA 6845, Australia
[b] Department of Geology and Geophysics, Yale University, New Haven, CT 06520-8109, USA
[c] Earth & Planetary Sciences/GEOTOP, McGill University, 3450 University St., Montreal, Quebec H3A0E8, Canada
[d] Tectonics, Resources and Exploration (TRaX), School of Earth and Environmental Sciences, University of Adelaide, SA 5005, Australia

ARTICLE INFO

Article history:
Received 6 January 2013
Received in revised form 24 May 2013
Accepted 28 May 2013
Available online 5 June 2013

Editor: J. Knight

Keywords:
Neoproterozoic
Rodinia
Gondwanaland
Glacial deposits
Snowball Earth
Palaeogeography

ABSTRACT

This review paper presents a set of revised global palaeogeographic maps for the 825–540 Ma interval using the latest palaeomagnetic data, along with lithological information for Neoproterozoic sedimentary basins. These maps form the basis for an examination of the relationships between known glacial deposits, palaeolatitude, positions of continental rifting, relative sea-level changes, and major global tectonic events such as supercontinent assembly, breakup and superplume events. This analysis reveals several fundamental palaeogeographic features that will help inform and constrain models for Earth's climatic and geodynamic evolution during the Neoproterozoic. First, glacial deposits at or near sea level appear to extend from high latitudes into the deep tropics for all three Neoproterozoic ice ages (Sturtian, Marinoan and Gaskiers), although the Gaskiers interval remains very poorly constrained in both palaeomagnetic data and global lithostratigraphic correlations. Second, continental sedimentary environments were dominant in epicratonic basins within Rodinia (>825 Ma to ca. 750 Ma), possibly resulting from both plume/superplume dynamic topography and lower sea-level due to dominantly old oceanic crust. This was also the case at ca. 540 Ma, but at that time the pattern reflects widespread mountain ranges formed during the assembly of Gondwanaland and increasing mean age of global ocean crust. Third, deep-water environments were dominant during the peak stage of Rodinia break-up between ca. 720 Ma and ca. 580 Ma, likely indicating higher sea level due to increased rate of production of newer oceanic crust, plus perhaps the effect of continents drifting away from a weakening superplume. Finally, there is no clear association between continental rifting and the distribution of glacial strata, contradicting models that restrict glacial influence to regions of continental uplift.

1. Introduction

After a billion years of Earth history devoid of evidence for continental ice sheets, glaciation occurred multiple times in the middle–late Neoproterozoic. The global distribution of Neoproterozoic glacial deposits, along with evidence that glaciers reached sea level in the low latitudes (see review by Evans and Raub, 2011, and references therein), present a major challenge to understanding the behaviour of the ancient Earth system. The repeated occurrence of tropical glaciation is a drastic departure from the Phanerozoic latitudinal zonal climatic patterns, where continental glaciations only occur in polar to moderate palaeolatitudes (Evans, 2003). Numerous models have been proposed to explain this phenomenon, the foremost of which is the Snowball Earth hypothesis (Hoffman et al., 1998). Palaeogeography, specifically the widely inferred low-latitude distribution of the continents in the middle Neoproterozoic, is central to the Snowball Earth. Joe Kirschvink, who first proposed this radical model, noted that "*a slight drop in sea level would convert large areas of energy-absorbing oceanic surface to highly reflective land surface, perhaps enhancing the glacial tendency*" (Kirschvink, 1992), thus potentially triggering a runaway feedback capable of causing the entire Earth to freeze over (Kirschvink, 1992; Hoffman et al., 1998; Hoffman and Schrag, 2002). The preferential low-latitude distribution of the continents could also have exerted other first-order controls on Earth's climate, most notably in the influence on silicate weathering. Higher precipitation rates on the low-latitude continents and, in particular, weathering of plume-induced continental flood basalts (Goddéris et al., 2003; Li et al., 2004) and continental fragmentation increasing proximity to moisture (Donnadieu et al., 2004) in the low latitudes should have enhanced silicate weathering and led to cooler global temperatures. Other potentially important factors of a low-latitude palaeogeography on global climate include enhanced carbon burial and methane clathrate genesis along newly formed shallow-marine passive margins (Schrag et al., 2002) and meridional

* Corresponding author at: ARC Centre of Excellence for Core to Crust Fluid Systems (CCFS) and The Institute for Geoscience Research (TIGeR), Department of Applied Geology, Curtin University, GPO Box U1987, Perth, WA 6845, Australia.
E-mail address: z.li@curtin.edu.au (Z.-X. Li).

0037-0738/$ – see front matter © 2013 Elsevier B.V. All rights reserved.
http://dx.doi.org/10.1016/j.sedgeo.2013.05.016

heat transport, which strongly influences conditions under which the Snowball runaway would initiate (Voigt and Abbo, 2012).

Evidence for thick accumulations of glacial sediments and at least transiently open water conditions (McMechan, 2000; Leather et al., 2002), have led some authors to support a less severe climatic scenario—the "slushball" or "soft Snowball"—where some seaways remained open near the palaeoequator (Hyde et al., 2000). An alternative to the Snowball Earth model that accounts for low latitude glaciation is the high obliquity (>54°) model, where high obliquity during the Precambrian resulted in a preferential low-latitude glaciation and strong seasonality on the equator (Williams and Schmidt, 2004). However, geodynamic models (Levrard and Laskar, 2003) and as-expected subtropical palaeolatitudes of Precambrian evaporite basins (Evans, 2006) suggest that Earth's obliquity has remained relatively consistent through Earth's history and render this model unlikely. Finally, the 'Zipper-rift' model attributes Neoproterozoic glacial deposits to high topography on rift shoulders and above plume-heads during the breakup of the supercontinent Rodinia (Eyles and Januszczak, 2004). That model sought to require no anomalous climatic conditions to account for the glacial record, but it does not explicitly account for the climatic implications of low-latitude ice sheets.

Critical for testing all of these models is the evolution of global palaeogeography during the Neoproterozoic, the timing and distribution of continental rift basins, basaltic magmatism, elevated land areas, and climate-diagnostic deposits such as glacial diamictites, carbonates and evaporites. We present in this paper a set of seven revised global palaeogeographic maps for the interval 825–540 Ma that illustrate mountains, shorelines, platforms, basins, and known climate-diagnostic deposits at key times in Neoproterozoic Earth history. This preliminary attempt to produce more key palaeogeographic maps with integrated palaeogeographic and stratigraphic information motivates a discussion of the geodynamic, geochemical, and palaeoclimatic implications of the evolving palaeogeography.

2. Methods

We choose seven time slices for our compilation: 825, 780, 720, 680, 635, 580, and 540 Ma. These time slices were chosen at ca. 50 Myr time intervals to coincide with three of the major Rodinian rifting episodes at ca. 825 Ma, 780 Ma and 720 Ma, the three major global glacial events at (approximately) ca. 720 Ma, 635 Ma and 580 Ma, and the final assembly of Gondwanaland at ca. 540 Ma (e.g., Li et al., 2008; Hoffman and Li, 2009). Important stratigraphic correlations that are used throughout our analysis include an assignment of ca. 720 Ma to the onset of the so-called "Sturtian" glaciation (Macdonald et al., 2010), and ca. 635 Ma to the end of the so-called "Marinoan" glaciation (Condon et al., 2005), although we recognise that the number, duration, and global significance of these events (e.g., Hoffman and Li, 2009, and references therein) remain highly debated. Most of the correlations we adopt are consistent with those presented by Hoffman and Li (2009), although we emphasise that many successions lack robust age control (Condon and Bowring, 2011). A third glacial interval known as the mid-Ediacaran or Gaskiers event, is dated at its type locality to ca. 580 Ma (Bowring et al., 2003) and is widely regarded to be only regional in extent (see Evans, 2000; Hoffman and Li, 2009; Evans and Raub, 2011). For the purpose of establishing correlations of 580 Ma strata in poorly dated basins or those lacking mid-Ediacaran glacial deposits, we assume that the Shuram carbon-isotope anomaly, which is expressed widely in un-glaciated continental margin deposits (Grotzinger et al., 2011), coincides with the Gaskiers ice age at ca. 580 Ma (Halverson et al., 2005), although this age assignment is poorly constrained, and many authors suggest an exclusively post-Gaskiers age for the Shuram event (e.g., Condon et al., 2005). Detailed descriptions of the Neoproterozoic glacial units and surrounding strata can be found in the recent compendium by Arnaud et al. (2011).

Our analysis is based on data from nearly 100 locations (see Supplementary Files I and II) across the various cratons, typically spaced at least several hundred km apart from each other (Fig. 1). The compilation of glacial deposits by Evans and Raub (2011) is a template for our approach, and our location index numbers are consistent with those used in that study. We have included several additional locations, which are listed by fractional index number in Supplementary File I. For each region and time slice, we choose a representative geologic unit (typically a Formation, but in places a Group) to indicate the palaeoenvironment and dominant lithology of rocks being deposited or formed in that region at that time. Most of these environments are sites of long-term accumulation of strata at the margins of cratons, because our compilation is biased toward regions with well-developed stratigraphic records. Presumably, the interiors of Neoproterozoic cratons, like those of today, were predominantly tectonically stable areas of low elevation and relief, but the lack of extensive stratigraphic records across those stable cratonic interiors has left them largely excluded from our analysis.

Within sites of enduring stratigraphic accumulation (Supplementary Files I and II), we classify depositional palaeoenvironments into four broad categories. *Intermontane terrestrial* refers to deposits interpreted to lie within small basins (molasse basins, grabens or perched rift basins) among otherwise eroding mountainous terrains. Such environments are rare in the geologic record and likewise are rare in our compilation. *Lowland terrestrial* represents the dominant mode of deposition that is interpreted as terrestrial, lacustrine, or in the case of volcanism, subaerial. *Shallow marine* indicates deposits with evidence for tidal or storm-influenced sedimentary features, microbialite buildups thought to lie within the photic zone, or other evidence indicative of accumulation on a continental shelf or platform. *Deep marine* indicates lack of such tidal or storm-influenced features, not specifying any particular water depth although most commonly interpreted as being deposited on the middle–outer shelf or continental slope, ca. 80 m or more below sea level. We also illustrate a dominant lithology to represent each region and age. We recognise that many successions comprise numerous intercalations of different lithologies and imprecise ages, and hence have endeavoured to pick the most characteristic lithology for each time interval. The names of these representative units are also given, so that our palaeogeographic maps can be updated most conveniently as new age constraints arise from the various regions.

In areas and times of active tectonism without sedimentary or volcanic deposition, we distinguish two classes of geologic record: plutonism and metamorphism. Where no such record is evident, and no sedimentary rocks are present for the particular region and age either due to non-deposition or due to erosion, disconformities are referred to generally as "unconformities" in Supplementary File I.

We updated our palaeogeographic reconstructions for the 825–540 Ma interval from the IGCP440 1100–530 Ma animation (Appendix II of Li et al., 2008), now taking into account the ca. 40° intraplate rotation between northern and southern Australia along the Paterson–Musgrave orogeny at 660–550 Ma (Li and Evans, 2011), and the "orthoversion" model for supercontinental transitions that locks absolute palaeolongitude of Rodinia to 100°E (Mitchell et al., 2012). We also corroborate our model with additional palaeomagnetic data acquired since 2007 (Table 1), the year when the IGCP440 working group decided upon a suitable set of reconstructions. These data include a pole from the ca. 570 Ma Nola dykes of the Congo craton (Moloto-A-Kenguemba et al., 2008), a new grand-mean pole from the Franklin large igneous province in northern Laurentia (Denyszyn et al., 2009), a revised pole from the Nantuo Formation in South China (Zhang et al., 2013), and poorly-dated but otherwise high-quality data from the Ediacaran of South Australia (Schmidt et al., 2009; Schmidt and Williams, 2010). We modified the position of India in Rodinia (Figs. 2, 3) by matching the ca. 1080 Ma Wajrakarur kimberlites pole (Miller and Hargraves, 1994) and the ca. 770 Ma Malani Rhyolite pole

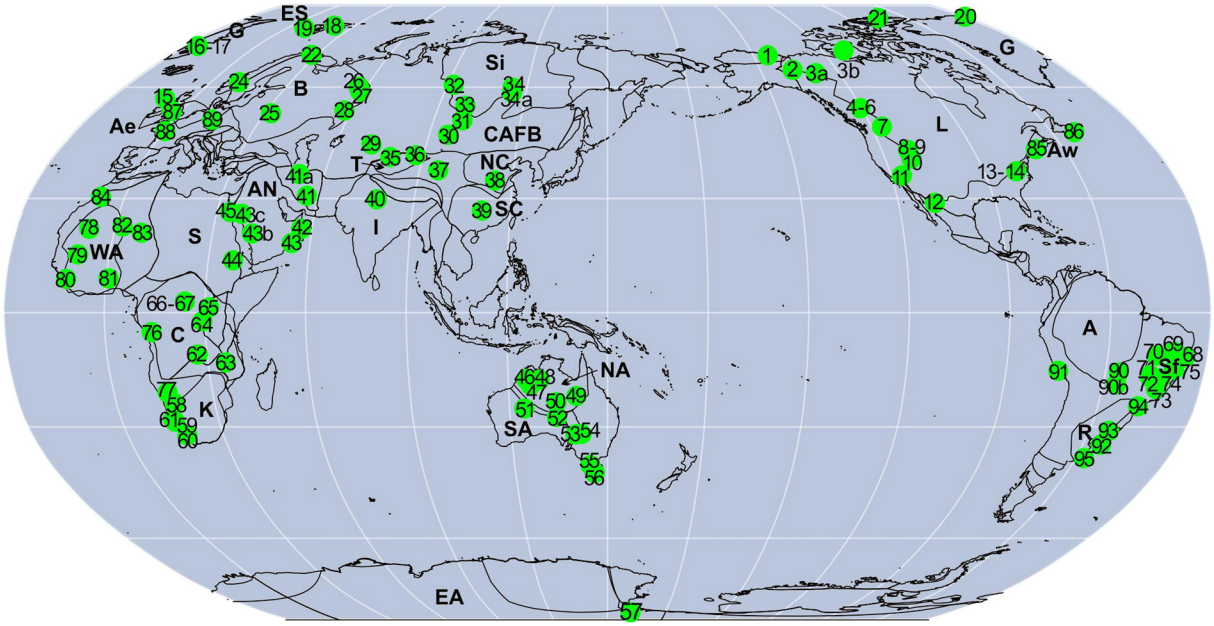

Fig. 1. Present location map for cratons and numbered sedimentary basin data points (marked in green circles) corresponding to the data points and tectonostratigraphic correlations in Supplementary File I—Table S1. Craton/terrane name abbreviations: A—Amazonia; Ae—Avalonia (east); AN—Arabia—Nubia; Aw—Avalonia (west); B—Baltica; C—Congo; CAFB—Central Asian Fold Belt; EA—East Antarctica; ES—East Svalbard; G—Greenland; I—India; K—Kalahari; L—Laurentia; NA—Northern Australia; NC—North China; R—Rio Plata; S—Sahara; SA—Southern Australia; SC—South China; Sf—Sao Francisco; Si—Siberia; T—Tarim; WA—West Africa.

(Gregory et al., 2009) with poles of corresponding ages from Laurentia and other continents (see Table 1 of Li et al., 2008). The relative position of South China in Rodinia follows that of the "Missing-Link" model (Li et al., 1995, 2008) (Figs. 2, 3), but its position relative to Australia after Rodinia breakup has been modified following new provenance results of Yao et al. (under review). The position of the Tarim Block broadly follows that of Li et al. (1996), but the orientation of the block has been modified using a new pole from the ca. 600 Ma Sugetbrak Formation (Zhan et al., 2007).

Supplementary File I also contains some data points from minor terranes, the precise positions of which within Rodinia are poorly known. These include data points 29–31 from the Central Asian Fold Belt (Supplementary File I and Fig. 1). In view of the general similarities between the tectonostratigraphic records of these locations and that of the Tarim Block, these terranes are notionally placed adjacent to northern or eastern Tarim blocks in our reconstructions. Data points 41–45 are from the Iranian Block and the Arabia–Nubian Shield (which itself consists of numerous different terranes that amalgamated during the Neoproterozoic; Stern and Johnson, 2010). We show these data points as part of the unexposed Sahara Craton adjacent to the Congo-São Francisco Craton.

We made our reconstructions with the GPlates software package (Williams et al., 2012) that incorporates continuous kinematics as an integral component of the reconstruction architecture; the time-slice maps herein are secondarily derived from our animated model. We strived for plate-tectonic realism in our kinematic model, in the sense that our reconstructions follow similar empirical "rules" as those apparent from reconstructions of the past 300 million years (Torsvik et al., 2008).

3. Results

The new palaeogeographic maps incorporate many tectonic, stratigraphic, and palaeoclimatic data, only some of which will be highlighted in the present contribution. References for the stratigraphic data are given in Supplementary File II, commonly without further elaboration. We recognise that chronostratigraphic correlations may be revised substantially in the future, and the joint publication of Supplementary File I with Figs. 1–8 is designed to facilitate updating of the reconstructions as new chronologic data are acquired. In addition, both the spatial and temporal density of the data entries (Supplementary File I) have the potential of being significantly enhanced so that more palaeogeographic time slices can be produced, and the palaeo-facies (thus palaeoenvironment) maps (Figs. 2–8) can be more precisely constrained. Below we describe each of the seven Neoproterozoic palaeogeographic snapshots between 825 Ma and 540 Ma (Figs. 2–8).

3.1. 825 Ma: mid-life Rodinia above a mantle superplume

The position of Rodinia at 825 Ma is about the same as that in the IGCP 440 map series (Li et al., 2008), but adjusted to take into account of ca. 40° rotation within Australia, and with India placed closer to northwestern Australia (see explanations in Section 2 of this paper). Rodinia extends from the palaeoequator to the polar region. We show a northern polar position for the high-latitude end of Rodinia, rather than the opposite south-polar option, because Laurentian apparent polar wander is thereby minimised between ca. 800 Ma and the semicontinuous 1.85–0.95 Ga path that is constrained at its older end by orographic effects in the trade wind belts (Hoffman and Grotzinger, 1993; Fig. 7 of Zhang et al., 2012).

One prominent global feature of the ca. 825 Ma world is the likely presence of a superplume under the northern(?) polar end of the supercontinent Rodinia (Li et al., 2003), and a possible antipodal superplume in the extra-Rodinian oceanic realm ("Mirovia"), analogous to the coexistence of the Pangaean (African) superplume and the antipodal Panthalassan–Pacific superplume during Pangaean time (Li et al., 2008; Li and Zhong, 2009). Li et al. (2008) attributed the formation of the antipodal superplumes to circum-supercontinent avalanches of subducted slabs to near the core–mantle boundary. Records of plume events on the polar end of Rodinia include the occurrence of mafic dyke swarms and large igneous provinces (Wingate et al., 1998; Li et al., 1999, 2003; Frimmel et al., 2001; Ernst et al., 2008; Wang et al., 2010), high-temperature mantle melts (Wang et al., 2007), regional doming (Li et al., 1999), tilting with accompanying erosion (Rainbird

Table 1
Palaeomagnetic poles used in this study (South poles in the model).

Craton/rock unit	Age (Ma)[a]	°N,°E	A95°	Pole reference
Laurentia				
Skinner Cove	551 ± 3	−15, 337	9	McCausland and Hodych (1998)
Sept-Iles A	565 ± 4	−20, 321	8	Tanczyk et al. (1987)
Catoctin A	572 ± 5	43, 298	18	Meert et al. (1994)
Callander syenite	577 ± 1	51, 283	8	Symons and Chiasson (1991)
Mutton Bay A	583 ± 2	43, 333	12	McCausland et al. (2011)
Grenville dykes B	590 ± 2	62, 250	14	Murthy (1971)
Long Range dykes (Labr)	615 ± 2	19, 355	17	Hodych et al. (2004)
Long Range dykes (Newf)	615 ± 2	06, 345	10	McCausland et al. (2009)
Franklin-Natkusiak	ca. 720	−08, 344	3	Denyszyn et al. (2009)
Kwagunt Fm	742 ± 6	−18, 346	7	Weil et al. (2004)
Tsezotene sills	779 ± 2	−02, 318	7	Park et al. (1989)
Wyoming dykes	ca. 784	−13, 311	4	Harlan et al. (1997)
Svalbard				
Svanbergfjellet	ca. 790 ?	−26, 047	6.0	Maloof et al. (2006)
Grusdievbreen upper	ca. 800 ?	01, 073	6.5	Maloof et al. (2006)
Grusdievbreen lower	ca. 805 ?	−20, 025	11.5	Maloof et al. (2006)
Baltica				
Winter Coast sedim.	555 ± 1	31, 293	10	Popov et al. (2002)
Egersund dykes	616 ± 3	31, 044	16	Walderhaug et al. (2007)
Hunnedalen dykes	ca. 850	41, 042	10	Walderhaug et al. (1999)
Amazonia				
Mirassol d'Oeste	635–580	−83, 293	7	Trindade et al. (2003)
West Africa				
Adma diorite	616 ± 11	33, 345	9	Morel (1981)
Congo				
Sinyai metadolerite	547 ± 4	−29, 319	5	Meert and Van der Voo (1996)
Nola metadolerite	571 ± 6	−62, 305	8	Moloto-A-Kenguemba et al. (2008)
Luakela volcanics B	ca. 580 ?	−38, 271	10	Wingate et al. (2010)
Mbozi complex	≥748 ± 6	46, 325	9	Meert et al. (1995) [a]
Luakela volcanics A	765 ± 7	40, 302	14	Wingate et al. (2010)
Gagwe lavas	795 ± 7	−25, 273	10	Meert et al. (1995)
Rio Plata				
Sierra Animas 2	ca. 580	−17, 251	18	Sánchez-Bettucci and Rapalini (2002)
Kalahari				
Gannakouriep	ca. 790	74, 238	6	Bartholomew (2008)
Australia (South + West frame >540 Ma)				
Upper Arumbera Sandst.	ca. 540	−44, 342	4	Kirschvink (1978)
Wonoka Fm	ca. 570 ?	−05, 031	5	Schmidt and Williams (2010)
Bunyeroo Fm	ca. 580 ?	−18, 016	9	Schmidt and Williams (1996)
Brachina Fm	ca. 615 ?	−46, 315	3	Schmidt and Williams (2010)
Nuccaleena Fm	ca. 635	−32, 351	3	Schmidt et al. (2009)
Elatina Fm	ca. 640	−44, 359	3	Schmidt et al. (2009)
Yaltipena Fm	ca. 650 ?	−44, 353	8	Sohl et al. (1999)
Mundine Well dykes	755 ± 3	−45, 315	4	Wingate and Giddings (2000)
Browne Fm	ca. 810 ?	−45, 322	7	Pisarevsky et al. (2007)
India				
Malani Rhyolite	ca. 770	−68, 253	9	Gregory et al. (2009)
South China				
Nantuo Fm	ca. 640	−09, 346	4	Zhang et al. (2013)
Liantuo Fm, CIT subset	<750	−03, 344	2	Evans et al. (2000) and this study
Xiaofeng dykes	802 ± 10	−14, 271	11	Li et al. (2004)
Tarim				
Sugetbrak Fm	ca. 600	−19, 330	9	Zhan et al. (2007)
Beiyixi volcanics	740–725	−18, 014	4.5	Huang et al. (2005); [a]
Aksu dykes	807 ± 12	−19, 308	6	Chen et al. (2004)
North China				
Nanfen Fm	ca. 790 ?	17, 301	11	Zhang et al. (2006)
Siberia (NW of Vilyuy-Patom axis)				
Kessyusa Fm	ca. 540	−38, 165	12	Pisarevsky et al. (1997)
Cisbaikalia redbeds	ca. 550 ?	−03, 168	8	Pisarevsky et al. (2000)
Shaman Fm	ca. 570 ?	−32, 071	10	Kravchinsky et al. (2001)
Biryusa dykes	613 ± 5	−25, 121	20	Metelkin et al. (2005)

[a] Ages are queried where highly uncertain or estimated in part by position on the APW path. Mbozi complex age from Mbede et al. (2004); Beiyixi volcanics ages from Xu et al. (2009); Mirassol d'Oeste age range given according to alternative correlations with dated glacial deposits on other cratons.

and Ernst, 2001), and continental rifting (Powell et al., 1994; Wang and Li, 2003). Locations of major continental rifts and anorogenic magmatism are shown in Fig. 2.

There are two notable features in Fig. 2 in terms of basin development. One is the scarcity of sedimentary record over the supercontinent Rodinia. Three major factors may have been at play. First, remnants of high topography (i.e., mountain ranges) that formed during the assembly of Rodinia between ca. 1100 Ma and 900 Ma (see orogens in Fig. 9a–d of Li et al., 2008) may still have existed at ca. 825 Ma. Second, doming above the Rodinian superplume and individual plumes, similar to the high elevation of present-day Africa above the African superplume, could have occurred for at least the high-latitude end of Rodinia.

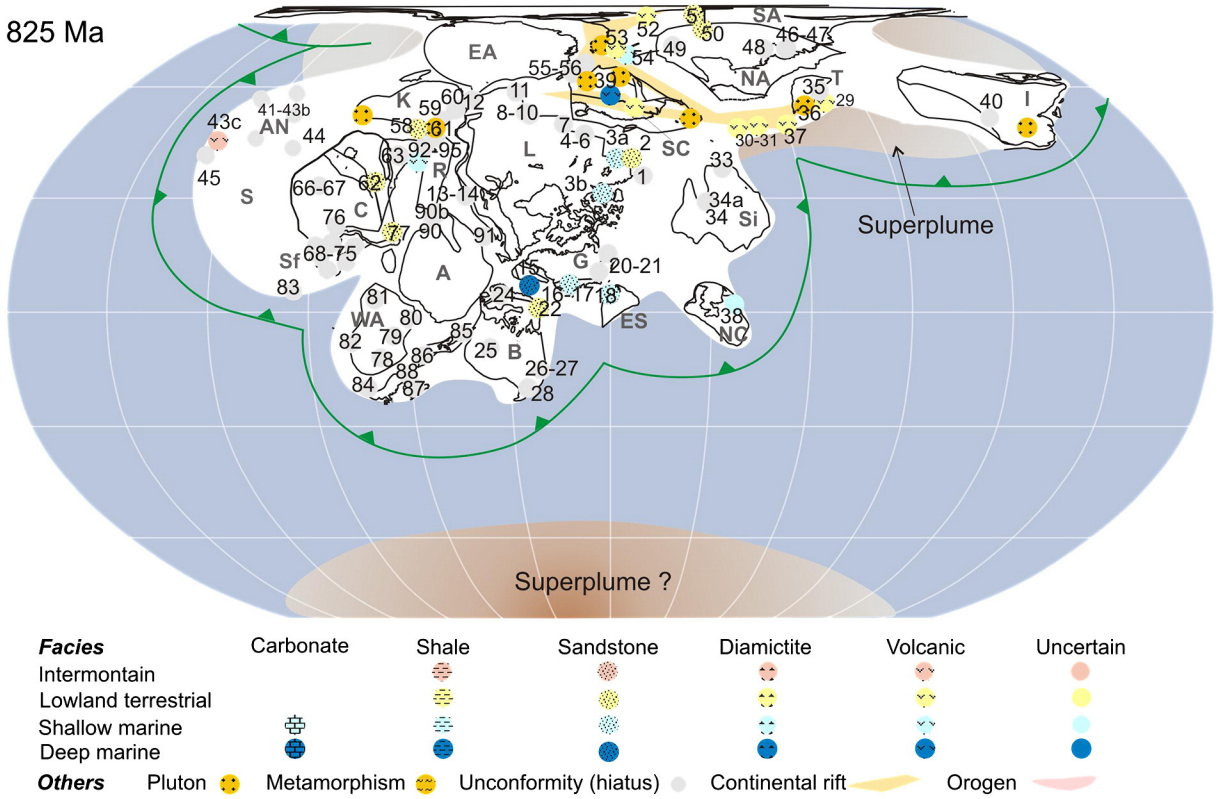

Fig. 2. Global reconstruction time-slice at 825 Ma, featuring a mid-life Rodinia stretching to the high latitude at above a mantle superplume, widespread erosion, and continental rifting. Craton/terrane name abbreviations are the same as for Fig. 1. Numbered tectonostratigraphic data points are the same as those shown in Fig. 1 with information given in Supplementary Files I and II. The legends shown here also apply to Figs. 3–8.

Third, the elimination of oceanic ridges between the continental blocks after the final assembly of Rodinia at ca. 900 Ma means a global reduction in the total volume of mid-ocean ridges, and therefore a net increase of total ocean volumes and thus a lower sea level (Russell, 1968; Valentine and Moores, 1970). The effect of supercontinent–superplume cycles on continental topography and sedimentation regimes will be discussed in greater detail in Section 4. Many of the sediments eroding from the supercontinent at this time would have been deposited along active margins and either subducted or subjected to high grade metamorphism and deformation.

Another notable feature is the lack of any glacial deposits despite the high-latitude position for parts of Rodinia and the presence of

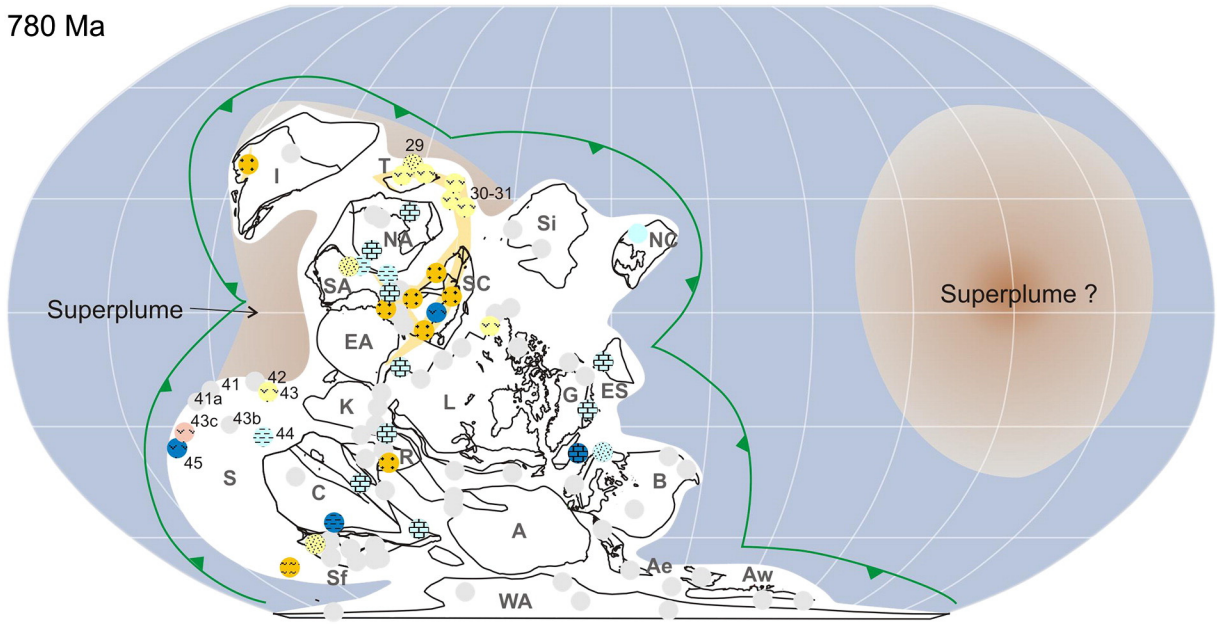

Fig. 3. Global reconstruction time-slice at 780 Ma featuring continued continental rifting on lower-latitude Rodinia.

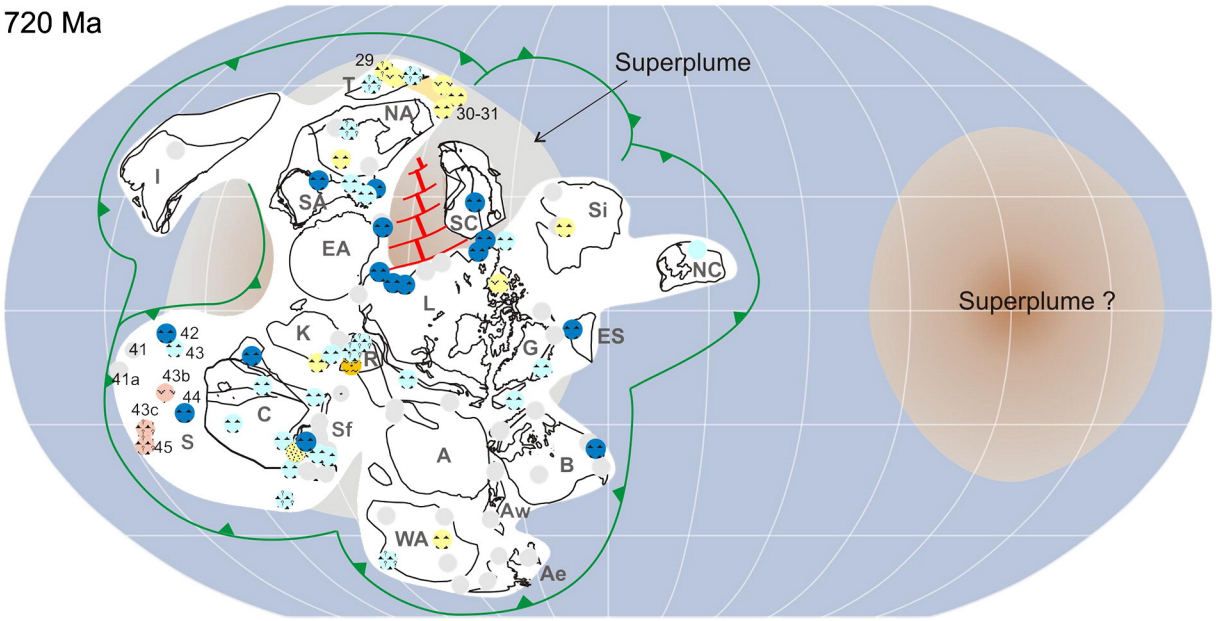

Fig. 4. Global reconstruction time-slice at 720 Ma, featuring the onset of Rodinia breakup, and pan-Rodinian "Sturtian" glaciation.

sedimentary basins there (e.g., in Australia). The reason for this anomaly is unclear, but is seems to represent a continuation of the preceding billion years for which there is no glacial record. More discussion on this will be provided in Section 4.

3.2. 780 Ma: continued continental rifting of low-latitude Rodinia

Li et al. (2004) reported palaeomagnetic evidence for a 90° rapid rotation of Rodinia between ca. 800 Ma and ca. 750 Ma around an Euler pole near the equator. They interpreted this rotation as a true polar wander (TPW) event caused by the non-equatorial positions of the antipodal superplumes at 825–800 Ma (Fig. 2). This hypothesis was partially supported by subsequent results from both East Svalbard (Maloof et al., 2006) and Australia (Swanson-Hysell et al., 2012), although those data require shorter and oscillatory TPW bursts. This sort of TPW behaviour might be explained in part by the "damping" effect of the rotational bulge and non-zero elasticity in the lithosphere (Creveling et al., 2012). Fig. 3 shows that by ca. 780 Ma, the bulk of Rodinia, as well as the hypothesised antipodal superplumes (Li et al., 2008; Li and Zhong, 2009), were already at low-latitude positions. It implies that if the large TPW event as suggested by Li et al. (2004) occurred at all, it was most likely between ca. 800 Ma and ca. 780 Ma, rather than lasting until ca. 750 Ma as originally thought.

Continental rifting continued in the northwestern half of Rodinia (in coordinates of the 780 Ma palaeogeography), but the southeastern half of Rodinia was still largely devoid of significant sedimentary basins. As such, continental to shallow marine deposits are relatively abundant in northwestern Rodinia at this time, but scarce over

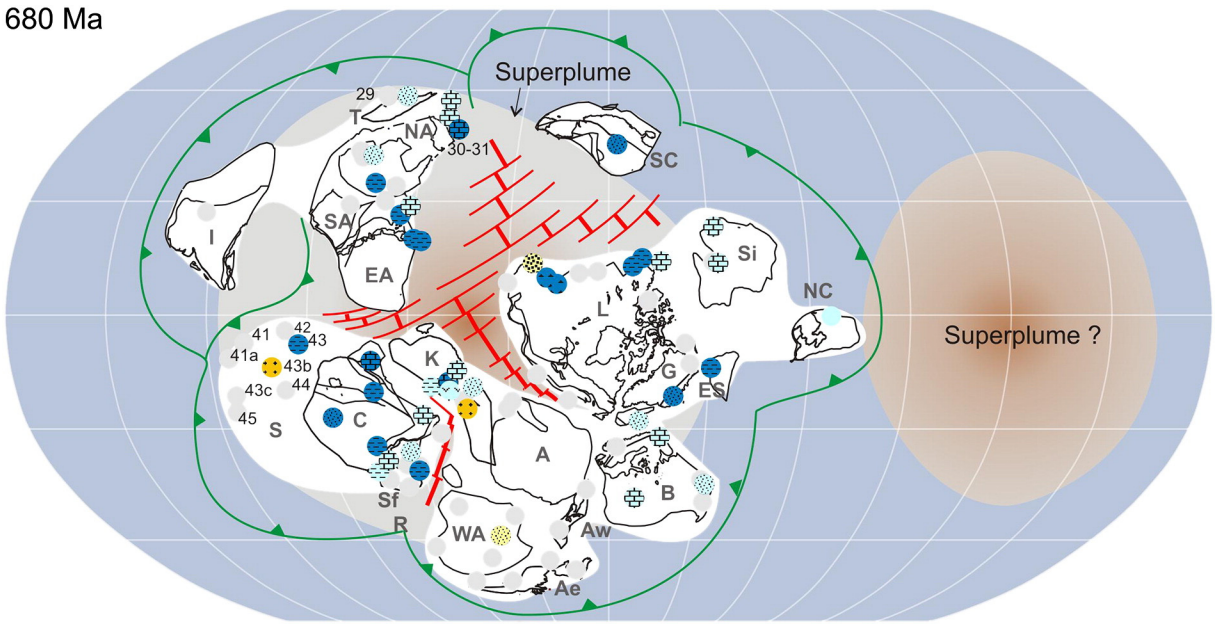

Fig. 5. Global reconstruction time-slice at 680 Ma: continuing Rodinia breakup and sea-level rises.

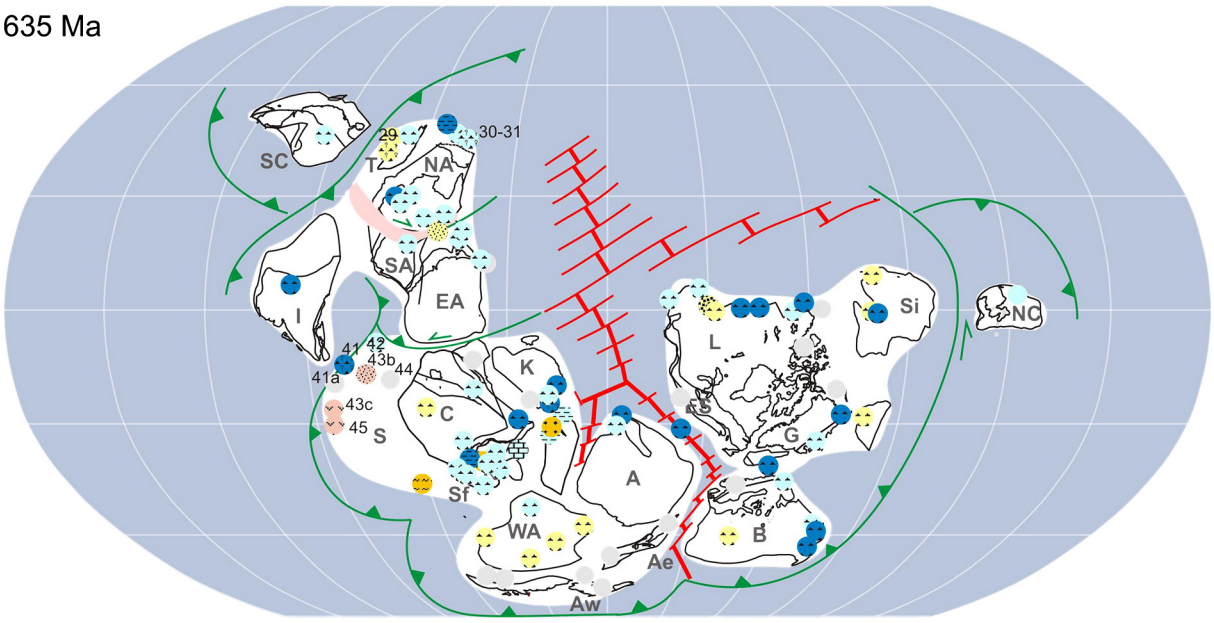

Fig. 6. Global reconstruction time-slice at 635 Ma: Rodinia breakup near completion, and the global "Marinoan" glaciation.

southeastern Rodinia, reflecting a strong asymmetry in the location of continental extension in Rodinia.

3.3. 720 Ma: onset of Rodinia breakup, and pan-Rodinian "Sturtian" glaciation

This reconstruction shows the palaeogeography at approximately the time of onset of Sturtian glaciation and temporally overlapping the emplacement of the Franklin large igneous province (Macdonald et al., 2010). A recent reanalysis of palaeomagnetic results, taking into account a ca. 40° intraplate rotation within Australia, suggests that Rodinia probably did not break up prior to 750 Ma as previously suggested (Wingate and Giddings, 2000); rather, the breakup likely occurred between the ca. 720 Ma onset of Sturtian glaciation and ca. 650 Ma (Li and Evans, 2011), even if continental extension presaging break-up had already begun some 100 million years earlier. We believe that South China started to break away at ca. 720 Ma (Fig. 4), assuming the Liantuo Formation palaeomagnetic pole is younger than the reported 750 Ma age, not only because it overlaps with the ca. 640 Ma Liantuo pole (Li and Evans, 2011), but also because of recent new age information for the formation. Despite a positive magnetostratigraphy test on the age of Liantuo palaeomagnetic remanence (Evans et al., 2000), there remains the possibility that the Sensitive High Resolution Ion MicroProbe (SHRIMP) date of 748 ± 12 Ma of the (Sturtian) Liantuo Formation tuff (Ma et al., 1984) was measured on xenocrystic zircons that are significantly older than the deposition age of the formation. Indeed, recent work found detrital zircons of ca. 730 Ma and ca. 700 Ma from the middle

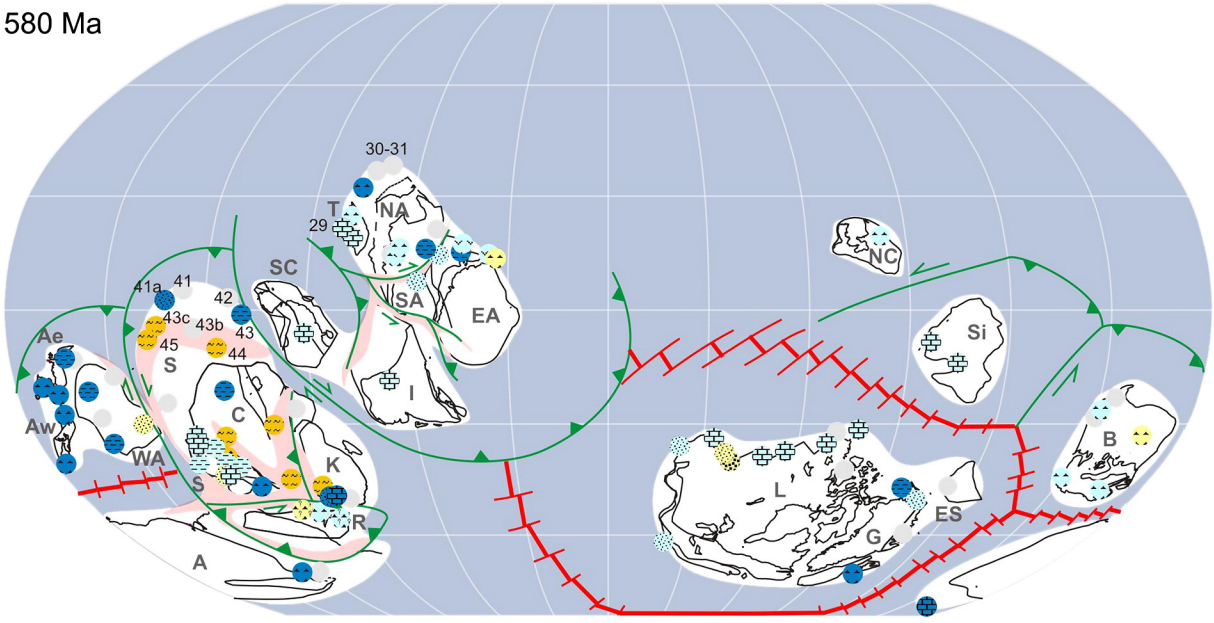

Fig. 7. Global reconstruction time-slice at 580 Ma featuring Rodinia breakup completion, early Gondwanaland assembly, and the "Gaskiers" glaciation.

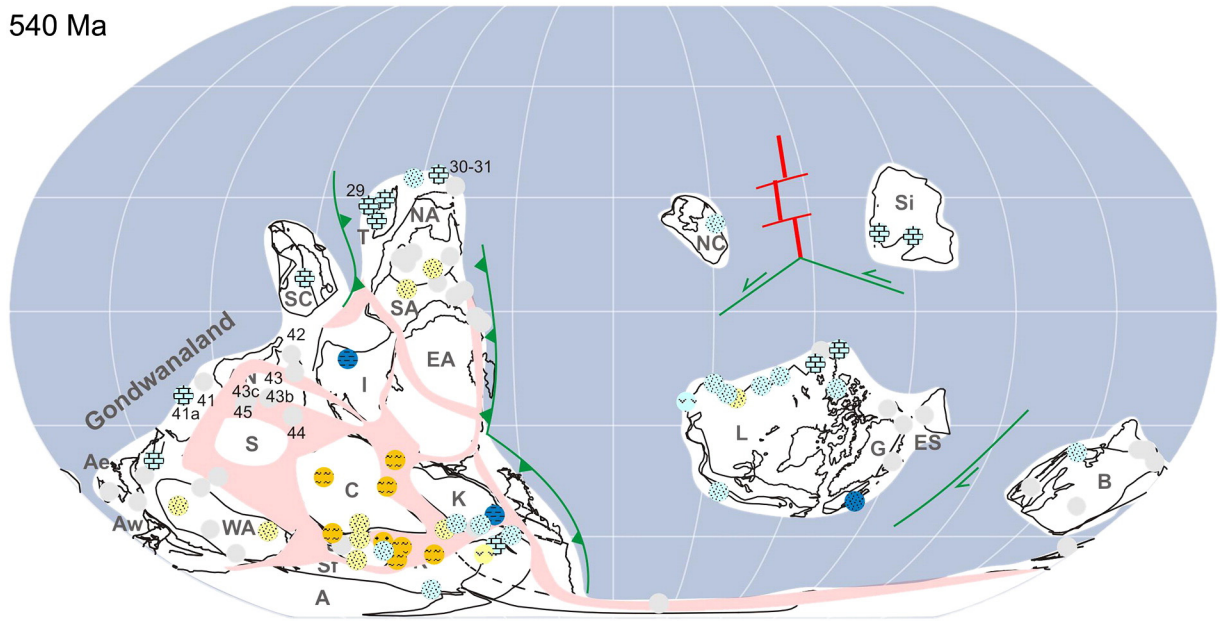

Fig. 8. Global reconstruction time-slice at 540 Ma featuring the formation of Gondwanaland, high continental topography, and the lowering of sea level.

and upper parts of a laterally correlative Liantuo succession, respectively (Liu et al., 2008), pointing to a possibly younger age and larger age range for the Liantuo Formation. We note that assigning a younger age to the Liantuo pole somewhat weakens the original argument by Li et al. (2004) for a ca. 90° TPW event. However, as discussed in the previous section, by accepting the Rodinia reconstruction we presented here, high-quality palaeomagnetic poles from Laurentia (e.g., Harlan et al., 1997) imply an earlier (by 780 Ma) completion of the 90° TPW event for Rodinia (Fig. 3).

One salient feature of the 720 Ma palaeogeography is the occurrence of glaciation, commonly at sea-level, throughout most of Rodinia. Glacial deposits on Rodinia spread across the entire latitude range of 60°N–60°S (Fig. 4), which is consistent with a Snowball Earth at that time. Definitive glacial deposits of Sturtian age are absent from India, Amazonia, and North China (Fig. 4), mainly due to the absence of a stratigraphic record from these cratons. However, in the case of the North China craton, shallow marine deposits with poorly constrained ages have been reported (Zhang et al., 2006). The absence of glacial deposits may reflect an incomplete stratigraphic record, or possibly isolation and submergence of the craton during glaciation.

Another feature of the 720 Ma palaeogeography is the apparent wider occurrence of epicontinental flooding, deep marine deposits in rift-marginal basins, and fewer depositional hiatuses (Fig. 4) when compared with earlier times (i.e., Figs. 2, 3, 9). This may partly reflect the further reduction of topographic relief associated with earlier orogenic events during the assembly of Rodinia, as well as continuing transgression caused by the maturing of continental rifts and creation of young oceanic lithosphere during the breakup of Rodinia.

3.4. 680 Ma: continuing Rodinia breakup

The process of continental breakup spread over much of Rodinia by ca. 680 Ma (Fig. 5). The two hypothesised antipodal superplumes were likely still active at that time, analogous to the Cretaceous during the breakup of Pangaea (Li and Zhong, 2009), with large igneous provinces (LIPs) developing both within the new oceans basins that opened between post-Rodinian continents, and above the superplume antipodal to the Rodinian superplume. This would have resulted in an increase in the proportion of young oceanic lithosphere and likely emplacement of LIP-related oceanic plateaus; together with the possible cessation and meltdown of the Sturtian glaciation, these factors likely caused a greater degree of deep marine deposition than at 720 Ma and earlier (Fig. 9). Our chronostratigraphic model generally treats all strata lying between the correlated "Sturtian" and "Marinoan" ice ages as coeval at ca. 680 Ma. An alternative model of the Sturtian ice age as enduring for about 50 million years (Rooney and Macdonald, 2012) would instead assign an age of ca. 650 Ma for most of the formations shown in Fig. 5, the only exceptions being those few with acceptable age constraints (e.g., Fulu Formation, South China). Aside from such minor exceptions, our map with a nominal age of 680 Ma could reasonably describe global palaeogeography of a post-Sturtian, pre-Marinoan world at ca. 650 Ma in the alternative, long-lived Sturtian ice age model.

3.5. 635 Ma: Rodinia breakup near completion, and the global "Marinoan" glaciation

The 635 Ma palaeogeography (Fig. 6) features the world at the end of the global "Marinoan" glaciation, again with glacial deposits spreading from >70° palaeolatitude to the palaeo-equator, and interpreted to represent a Snowball Earth event (Hoffman et al., 1998; Hoffman and Schrag, 2002). Glacial deposits of this age have been found on all major continental blocks except for the North

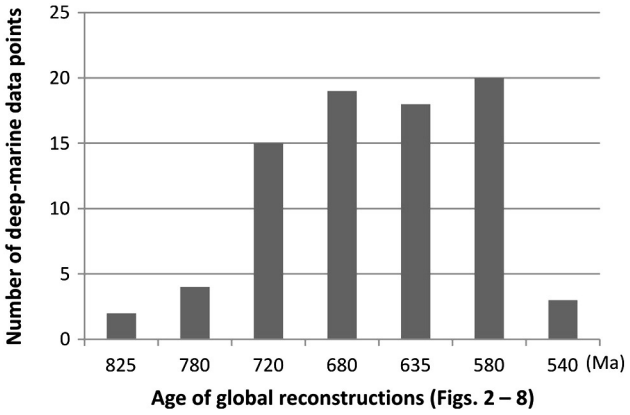

Fig. 9. Variations in the number of regions subject to deep marine environments during each of the seven palaeogeographic snap shots (Figs. 2–8, and Supplementary File I).

China craton, again possibly because of its isolated position and total submergence. Apart from Siberia and Baltica, all other continents had separated from Laurentia. Northern Australia had begun its counterclockwise rotation relative to southern Australia (Li and Evans, 2011).

We did not show the two antipodal superplumes from this time onward, because although they may still have existed, they were likely significantly weakened due to the disintegration of the supercontinent-girdling subduction system, which had earlier dominated the mantle convection system along with the complementary, antipodal superplumes (Li et al., 2008; Li and Zhong, 2009). Post-breakup reduction in the extent of those Rodinian superplumes, and presumed relationship to inferred large, lower-mantle shearwave-velocity provinces (LLSVPs) conforms to the general model of their intimate connection with the supercontinent cycle (Li and Zhong, 2009; Evans, 2010; Mitchell et al., 2012) rather than their longevity through billions of years of Earth history (Burke et al., 2008; Dziewonski et al., 2010; Torsvik et al., 2010; Burke, 2011).

3.6. 580 Ma: Rodinia breakup completion, early Gondwanaland assembly, and the "Gaskiers" glaciation

The palaeogeographic reconstruction at 580 Ma, in mid-Ediacaran time, departs the most from the IGCP 440 map series (Appendix II of Li et al., 2008). The new map incorporates the high-latitude option for Laurentia, and the application of the new ca. 570 Ma Nola dykes palaeomagnetic pole from the Congo craton (Moloto-A-Kenguemba et al., 2008) that brought the West Gondwanaland continents to much lower palaeolatitudes (Fig. 7). We emphasise that this reconstruction is the least well palaeomagnetically-constrained in this map series, and should therefore be treated with caution. Even among cratons with many relatively robust palaeomagnetic data, such as Laurentia, there remains substantial disagreement over palaeolatitudes within the quality-filtered dataset (e.g., McCausland et al., 2011), forcing either exclusion of one group versus another (Pisarevsky et al., 2008), consideration of very rapid plate tectonics (Meert and Tamrat, 2004), proposal of rapid true polar wander (Mitchell et al., 2011), or a radically different geomagnetic field behaviour (Abrajevitch and Van der Voo, 2010). This important issue remains unresolved.

In this reconstruction, Rodinian breakup was complete by 580 Ma, as seen in the complete isolation of Laurentia from all other continents. We show South China colliding with India at this time, as recently proposed by Yao et al. (under review) based on its strong provenance connection with the High Himalaya from around that time until the Lower Palaeozoic. West Gondwanaland was largely formed by this time, and East Gondwanaland was also nearly assembled.

The "Gaskiers" glacial deposits, although not as widespread as those of the previous two glaciations, are still found on numerous continents: Baltica, Laurentia, North China, Australia, Tarim, Avalonia (marginal to West Africa), Congo-São Francisco, and Amazonia. Their depositional environments range from continental basins, shallow marine, to deep marine, and their palaeolatitudes, as shown on the reconstruction, spread from relatively high latitude (ca. 70° for Amazonia) to near the palaeo-equator (Australia and Avalonia). This wide latitudinal distribution of Gaskiers glacial deposits is consistent with "Snowball Earth" glaciation. However, the short duration of glaciation suggested by U—Pb zircon TIMS ages from the type locality in Newfoundland (Condon and Bowring, 2011) and the lack of distinct cap carbonate sequences associated with middle Ediacaran glaciation (Halverson et al., 2005) seem incompatible with a "hard Snowball" model. This inconsistency suggests that the Gaskiers glaciation may prove critical in understanding Neoproterozoic climate and the transition from global Cryogenian glaciations to Phanerozoic-type ice ages.

3.7. 540 Ma: final assembly of Gondwanaland, high continental topography, and the lowering of sea level

The final assembly of Gondwanaland (Fig. 8) took place through the formation of a network of orogens girdling the cratons that make up present day Africa (the so-called "Pan-African orogens"). Counterclockwise rotation between north and south Australia was completed by about 550 Ma (Li and Evans, 2011). South China was still rotating against the northwestern margin of Gondwanaland (Li, 1998; Li and Powell, 2001), and an Andean-type active margin developed along the palaeo-Pacific margin of Gondwanaland. Laurentia, Baltica, Siberia and North China were all isolated within palaeo-oceans, with North China drifting toward Australia to join East Gondwanaland by mid- to late Cambrian (McKenzie et al., 2011).

Much of Gondwanaland was elevated due to the extensive continental collision, hence erosion and terrestrial deposition were widespread (Fig. 8). Some of the large amount of eroded materials are preserved as siliciclastic sandstone in northern Africa (e.g., Avigad et al., 2005), across the Himalaya (Myrow et al., 2010), South China (Yao et al., under review), and eastern Australia (Squire et al., 2006; Veevers et al., 2006). Late Ediacaran seawater strontium isotope compositions likely reflect this extensive erosion in a final significant increase in $^{87}Sr/^{86}Sr$, following a prior long-term rise in the Neoproterozoic (Halverson and Shields-Zhou, 2011). Campbell and Allen (2008) invoked both extensive erosion of mountain belts and the corresponding voluminous deposition of carbonaceous and pyritic sediment as central drivers in the rapid oxidation of the Earth's atmosphere and presumably closely linked rapid evolution of complex life from the Ediacaran to Cambrian periods.

Another notable feature of the 540 Ma palaeogeography is the abundance of deep marine deposits, in contrast with the previous four time slices (Fig. 9). Apart from the elevated topography within Gondwanaland caused by the many young orogens, another factor that may have contributed to this pattern might be eustatic sea level fall due to ageing of oceans basins formed during the complete breakup of Rodinia some 50 million years earlier.

4. Discussion

The series of new plate reconstructions for key time slices in the Neoproterozoic presented herein represents an evolution from previous plate reconstruction models (e.g., Li et al., 2008), with some important revisions based on new palaeomagnetic and radiometric data. The principal additions to our maps are accurately reconstructed lithological data from the abundant Neoproterozoic sedimentary record (Supplementary Files I and II). The underlying motivations in adding this new layer of information to our paleogeographic maps are threefold. First, it serves as a basic geological check on the feasibility and validity of the reconstructions. Second, it should help inform debates and models regarding Neoproterozoic Earth system evolution, specifically the nature of Rodinia break-up and glaciations. Third, we intend for this preliminary compilation of lithological data to crystallise the construction of a more thorough Neoproterozoic stratigraphic database, to provide more detailed and quantitative tests of reconstructions and guide future research into Neoproterozoic palaeogeography and its implications.

The current compilations raise several key questions that either point to problems with the reconstructions or shortcomings in our understanding of how the Neoproterozoic Earth behaved. In either case, consideration of these problems will help us to better understand and frame the debate over Neoproterozoic palaeogeography.

4.1. Evaporites at 825 Ma?

The plate reconstruction for 825 Ma shows a Rodinia supercontinent occupying the northern hemisphere, with a cluster of continents

straddling the North Pole (Fig. 2). This reconstruction, however, may fail an important geological test. Evans (2006) previously demonstrated that most major evaporite sequences in the stratigraphic record were deposited in the sub-tropics, including Proterozoic occurrences. However, widespread evaporites were being deposited ca. 825 Ma in several basins (Evans, 2006), notably the Officer basin in Australia (data point 51), the Mackenzie Mountains in northwest Canada (data point 3), and the Amundsen basin in northern Canada (Rainbird et al., 1996), all of which are located in the high latitudes on Fig. 2. Because direct palaeomagnetic constraints on these units or conformably associated strata imply deposition in the sub-tropics (Evans, 2006), this inconsistency implies either that our reconstruction model is flawed or that the evaporites do not correlate in age to independently dated formations that have yielded the high-latitude palaeomagnetic data. Given the poor radiometric age control for the early Neoproterozoic, it is likely that the latter explanation at least partly accounts for this problem. However, this inconsistency can also be resolved if the ca. 800 Ma TPW event, rather than being a one-way trip as initially surmised (Li et al., 2004), was in fact an oscillatory pair of events, whereby Rodinia transited from the low latitudes to middle–high latitudes and back again (Maloof et al., 2006; Swanson-Hysell et al., 2012). In this case, the evaporites would have been deposited in the low-latitudes prior to or during the first phase of the TPW oscillation, and the high-latitude configuration shown in Fig. 2 would represent only a transient paleogeography.

4.2. 825–720 Ma climatic clues and conundrums

As noted above, despite the expansive continental area at high latitudes, no sediments representing glacial conditions have been reported at ca. 825 Ma (or ca. 800 Ma either, for that matter, if the transient mid-TPW interpretation is applied to Fig. 2 as discussed above). Given the relatively extensive sedimentary record for this time period, in particular in northern Laurentia, South China, and Australia (Fig. 2), it seems unlikely that such deposits have merely been overlooked; it is reasonable to conclude instead that the early Neoproterozoic enjoyed a stable, non-glacial climate. The subsequent 780 Ma time slice (Fig. 3) places much of the opposite end of Rodinia in the high southerly latitudes, straddling the South Pole. Although the paucity of high-latitude sedimentary basins at this time renders the stratigraphic record less conclusive in eliminating the null hypothesis that there was no glaciation at this time, it nevertheless stands out as a stark contrast to the subsequent 720 Ma time slice where glacial deposits are widespread across a dominantly low-latitude supercontinent (Fig. 4).

Previous authors have argued that pCO_2 levels across the Mesoproterozoic–Neoproterozoic transition were roughly 10× greater then present atmospheric levels based on a combination of the muted fluctuations in $\delta^{13}C$ in marine carbonates (signalling a larger DIC reservoir; Bartley and Kah, 2004) and the occurrence of calcifying cyanobacteria dating back to ca. 1200 Ma (Kah and Riding, 2007). The relatively abrupt onset of global glaciation at ca. 720 Ma corresponds to a potentially unique time in the Neoproterozoic when there were few high-latitude continents and possibly none at the poles (Fig. 4). This observation strengthens the popular argument that palaeogeography plays a first order role in determining Earth's stable climatic state. Two notable differences between the 825 and 720 Ma palaeogeographies within this context are 1) the middle–high versus tropical–middle palaeolatitude distribution of the continents; 2) and the onset of break-up of Rodinia by 720 Ma, with the opening of new ocean basins. Less obvious in the reconstructions but also possibly very important would have been the occurrence of several vast flood basalts associated with the superplume under northern Rodinia, notably the ca. 825 Ma Willouran-Guibei (Australia and South China; Wang et al., 2010), 780 Ma Gunbarrel (NW Laurentia; Harlan et al., 2003), and ~720 Ma Franklin (northern Laurentia; Denyszyn et al., 2009) large igneous provinces.

Godderis et al. (2003) argued that extrusion and subsequent weathering of a large flood basalt province in the tropics could trigger Snowball glaciation due to high weatherability of mafic rocks. The Franklin LIP was emplaced at low-latitudes (Denyszyn et al., 2009) and temporally overlaps the onset of Sturtian glaciation (Macdonald et al., 2010), implying a link between the two events. We note that in our 720 Ma reconstruction, the Franklin LIP would have straddled the equator, in direct line of oceanic moisture from the easterly trade winds, with no obvious intervening mountain belts. Hence, the basaltic plateau, along with 825–750 Ma basaltic plateaux in other parts of Rodinia (e.g., Kalahari, South China, Australia and Laurentia; see Fetter and Goldberg, 1995; Li et al., 1999, 2003, 2008; Barovich and Foden, 2000; Frimmel et al., 2001; Harlan et al., 2003; Ernst et al., 2008; Wang et al., 2011), would have been highly prone to chemical weathering, making it a powerful sink of atmospheric CO_2. However, this link remains conjectural, and discerning the potential and relative roles of basalt weathering, low-latitude palaeogeography, and a rifting supercontinent will require a combination of higher-resolution and better-calibrated chemostratigraphic data sets of proxies sensitive to continental weathering than are currently available (e.g., Halverson et al., 2010), as well as more powerful biogeochemical and climatic models.

4.3. Low-latitude glaciation and the Snowball Earth hypothesis

Low-latitude glaciation is the cornerstone of the Snowball Earth hypothesis (Kirschvink, 1992; Hoffman et al., 1998). Because most energy balance models show only one stable climatic state with continental glaciers in the low-latitudes (Ikeda and Tajika, 1999), the evidence for tropical glaciers in tide water for both the Sturtian (Denyszyn et al., 2009; Macdonald et al., 2010) and Marinoan (Sohl et al., 1999) ice ages presents strong support for such a globally engulfing “Snowball” state. Another key element of the Snowball hypothesis is that the glaciations should have been long-lived (up to tens of millions of years) in order for atmospheric CO_2 concentrations to build to the levels required to overcome the high-albedo effect of low-latitudes glaciation and trigger melting (Caldeira and Kasting, 1992; Hoffman et al., 1998; Pierrehumbert, 2004).

The two pillars of the Snowball hypothesis offer a straightforward test of the Snowball hypothesis: evidence for short-lived, low-latitude glaciation could falsify the hypothesis. The occurrence of low latitude glaciations during the Neoproterozoic is now commonly accepted (Figs. 4, 6, 7, 10). However, estimating the durations of these glacial events is more challenging because of sparse geochronological data. The exception is the middle Ediacaran Gaskiers glaciation, where in the type area on the Avalon Peninsula, Newfoundland, precise TIMS U—Pb zircon dates appear to constrain its duration to ≤2.6 m.y. (Condon and Bowring, 2011). Indeed, the short duration of the Gaskiers glaciation has commonly been regarded as evidence that it was not a Snowball glaciation (e.g., Halverson, 2006). If ice sheets really expanded from the middle–high latitudes to the tropics during the Gaskiers event, as implied by the ca. 580 Ma reconstruction (Figs. 6, 10), then this poses a serious challenge to the “hard” Snowball Earth hypothesis for that time interval and, more broadly, our understanding of ancient glacial climates. However, middle Ediacaran glaciation remains poorly understood, and it has not yet been established that there was a single (Gaskiers) glaciation, versus multiple glaciations or pulses. Because the middle Ediacaran palaeogeography is also the most poorly constrained of our reconstructions, and since this interval is variably associated with fast continental motions (Meert and Tamrat, 2004), rapid true polar wander (Mitchell et al., 2011), or a non-actualistic geodynamo (Abrajevitch and Van der Voo, 2010), we caution against drawing strong conclusions about the behaviour of the Neoproterozoic Earth system based on this reconstruction alone. Instead, it should motivate attempts to

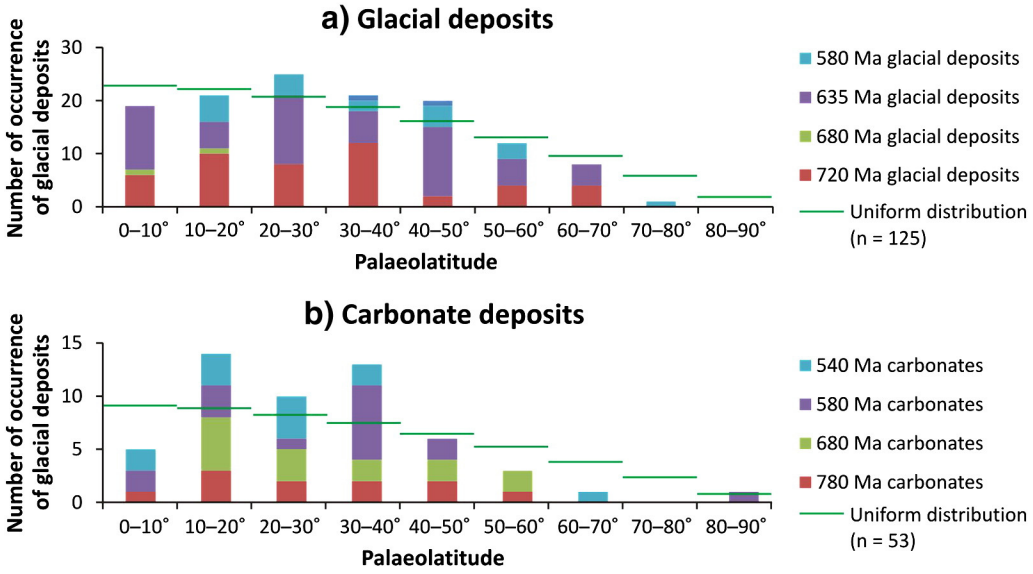

Fig. 10. Palaeolatitudinal distribution of glacial deposits (a) and carbonate deposits (b) according to our palaeogeographic reconstructions (Figs. 2–8) and Supplementary File I.

test the reconstruction and establish more firmly and precisely the timing and palaeogeography of middle Ediacaran glaciation.

4.4. A connection between rifts and glaciation?

Whereas some glacial units were clearly laid down in rift environments, our synoptic view of the global Neoproterozoic stratigraphic and tectonic regimes indicates that there is no predominant association between glaciation and continental rifting. This conclusion contradicts the "zipper-rift" hypothesis of Eyles and Januszczak (2004), in which Neoproterozoic ice ages are attributed to glaciation nucleated on rift shoulders developed during the break-up of Rodinia. The analysis of Eyles and Januszczak (2004) was based on a limited dataset that disregarded robust palaeomagnetic evidence for low-latitude glacial deposits (Evans, 2000; Evans and Raub, 2011). It is clear both from available data and from our 720 Ma (Fig. 4) and 635 Ma (Fig. 6) reconstructions that multiple, stable, tropical platforms were glaciated during the Cryogenian ice ages. Simply put, Cenozoic palaeoclimate is not an adequate analog for the Cryogenian.

4.5. Relative sea-level changes: controlled by supercontinent–superplume cycles?

Paucity of deep marine depositional environments typifies epicratonic stratigraphy during Rodinia time (Figs. 2, 3, 9), and this may result from plume/superplume dynamic topography, plus lower eustatic sea level, due to dominantly old oceanic crust. Conversely, deep marine depositional environments were much more widespread during the breakup of the supercontinent Rodinia, interpreted to reflect relative sea-level rise due to reduced ocean basin volume (Figs. 4–7, 9). This could have been caused by the formation of new mid-ocean ridges during supercontinental breakup, and also by formation of new oceanic plateaux above various Rodinia mantle plumes or superplumes in the new oceans. The drifting of continental blocks away from the centre of the Rodinian superplume during supercontinental breakup may also have contributed to the increased occurrence of relatively deep-water environments within the subsiding sedimentary repositories. Deep-water deposition diminished again by 540 Ma (Figs. 8, 9), once more indicative of continental collisions and old ocean basins.

The effect of supercontinent cycles on sea level changes was first recognised by Russell (1968) and Valentine and Moores (1970) largely based on the observation of first-order sea-level changes during the Pangaean cycle: global sea-level lowers during supercontinent time in responding to an increased ocean basin volume, and global sea-level rise during supercontinent breakup in responding to the addition of new oceanic ridges between parting continental fragments and thus a reduction in the total volume of the ocean basins. More recent work (e.g., Miller et al., 2005) confirmed a sea-level drop and a trough in the percentage of flooded continents during Pangaean time (ca. 320–170 Ma) and a significant sea-level rise and a peak in the percentage of flooded continents during the Late Jurassic–Cretaceous breakup of Pangaea. Muller et al. (2008) further demonstrated from a geodynamic point of view that the mean age of the world's ocean crust was over 20 Myr younger in the Cretaceous (the peak-time of Pangaea breakup) than that of the present-day oceans, corresponding to a sea-level 170 m higher than it is today. Zhang et al. (2012) simulated the effect of supercontinent–superplume cycles (e.g., Li and Zhong, 2009) on the continental topography and sea-level changes, including topographic highs over superplumes. Our observations for the 825 Ma–540 Ma Rodinia cycle, as discussed above, are consistent with those observed for the Pangaean cycle and geodynamic modelling results.

4.6. Carbonates and the background Neoproterozoic climatic state.

It is gratifying to observe extensive carbonate deposits, typically thought to indicate warm-water conditions both from a thermodynamic and biologic standpoint, deposited predominantly in low palaeolatitudes in our palaeogeographic reconstructions (Fig. 10b). Along with the record from evaporite basins, some discussion of which is presented above in Section 4.1, the typical low-palaeolatitude association of carbonates serves as a simultaneous test of kinematic models and climatic uniformitarianism in deep time. Extensive deposition of carbonates on epicontinental or post-Rodinian passive margins outside of the three glacial intervals (Figs. 2, 3, 5, 8) accords with a background "greenhouse" climate state and high pCO_2 levels inferred by various geochemical proxies as noted above. The late Neoproterozoic ice ages appear to have been nonuniformitarian paleoclimatic departures from that generally benign background state.

5. Conclusions

We present here a set of updated global palaeogeographic maps for the 825–540 Ma interval, decorated with dominant sedimentary facies

for selected stratigraphic sections from all major continents, and major orogenic belts and continental rift systems. Though the reliability of our maps are constrained by the availability of high-quality palaeomagnetic data (Table 1), as well as the limited number of stratigraphic data points that we were able to utilise for this work (Supplementary Files I and II), there are nonetheless a number of important observations:

(1) No glacial deposits have been found in the ca. 825 Ma world despite the high-latitude position for parts of Rodinia and the presence of sedimentary basins there (e.g., in South China and Australia), likely reflecting a pre-800 Ma atmosphere significantly different from that after 800 Ma.
(2) Low-latitude glacial deposits (near sea level) appear to extend from high latitudes into the deep tropics for all three ice ages (Sturtian, Marinoan, Gaskiers), which is consistent with Snowball Earth-type models.
(3) Deep marine depositional environments are notably sparse during Rodinia time (Figs. 2, 3), likely reflecting plume/superplume dynamic topography, lower sea level due to relatively old (on average) oceanic crust after supercontinent assembly, and the paucity of passive margins. Diminishing deep-water deposition dominated again at 540 Ma, once more indicative of continental collisions and old ocean basins.
(4) The increased prevalence of deep-water depositional palaeoenvironments during Rodinia break-up (720 Ma to 580 Ma), appears to indicate higher sea level due to the increasing amount of newer oceanic crust, possible presence of a large number of oceanic plateaus in the newly formed oceans, plus perhaps the effect of continents drifting off a weakening sub-supercontinent superplume.
(5) Whereas some glacial units were clearly laid down in rift environments, our synoptic view of the global Neoproterozoic stratigraphic and tectonic regimes indicates that there is no predominant association between glaciation and continental rifting.

Acknowledgements

This work was supported by the Australian Research Council grants DP770228, DP110104799, the Centre of Excellence for Core to Crust Fluid Systems (CCFS), NSERC (GPH). Both Curtin and Yale universities supported a three-month study leave by ZXL at Yale University, which stimulated this contribution. We thank two anonymous reviewers and Editor in Chief Jasper Knight for constructive reviews. This is TIGeR (The Institute for Geoscience Research) publication 466, and contribution 314 from the ARC Centre of Excellence for Core to Crust Fluid Systems (http://www.ccfs.mq.edu.au).

Appendix A. Supplementary data

Supplementary data to this article can be found online at http://dx.doi.org/10.1016/j.sedgeo.2013.05.016.

References

Abrajevitch, A., Van der Voo, R., 2010. Incompatible Ediacaran paleoomagnetic directions suggest an equatorial geomagnetic dipole hypothesis. Earth and Planetary Science Letters 293, 164–170.
Arnaud, E., Halverson, G.P., Shields-Zhou, G., 2011. The Geological Record of Neoproterozoic Glaciations. Geological Society of London, Memoir, 36 (735 pp.).
Avigad, D., Sandler, A., Kolodner, K., Stern, R.J., McWilliams, M., Miller, N., Beyth, M., 2005. Mass-production of Cambro-Ordovician quartz-rich sandstone as a consequence of chemical weathering of Pan-African terranes: environmental implications. Earth and Planetary Science Letters 240, 818–826.
Barovich, K.M., Foden, J., 2000. A Neoproterozoic flood basalt province in southerncentral Australia: geochemical and Nd isotope evidence from basin fill. Precambrian Research 100, 213–234.
Bartholomew, L.T., 2008. Paleomagnetism of Neoproterozoic intraplate igneous rocks in the southwest Kalahari craton, Namibia and South Africa. Unpublished Bachelor's Thesis The University of Texas at Austin (174 pp.).
Bartley, J.K., Kah, L.C., 2004. Marine carbon reservoir, C_{org}—C_{carb} coupling, and the evolution of the Proterozoic carbon cycle. Geology 32, 129–132.
Bowring, S., Myrow, P., Landing, E., Remezani, J., Grotzinger, J., 2003. Geochronological constraints on terminal Neoproterozoic events and the rise of metazoans. Geophysical Research Abstracts 5, 13219.
Burke, K., 2011. Plate tectonics, the Wilson cycle, and mantle plumes: geodynamics from the top. Annual Reviews of Earth and Planetary Sciences 39, 1–29.
Burke, K., Steinberger, B., Torsvik, T.H., Smethurst, M.A., 2008. Plume generation zones at the margins of large low shear velocity provinces on the core–mantle boundary. Earth and Planetary Science Letters 265, 49–60.
Caldeira, K., Kasting, J.F., 1992. Susceptibility of the early Earth to irreversible glaciation caused by carbon dioxide clouds. Nature 359, 226–228.
Campbell, I.H., Allen, C.M., 2008. Formation of supercontinents linked to increases in atmospheric oxygen. Nature Geosci 1, 554–558.
Chen, Y., Xu, B., Zhan, S., Li, Y., 2004. First mid-Neoproterozoic paleomagnetic results from the Tarim Basin (NW China) and their geodynamic implications. Precambrian Research 133, 271–281.
Condon, D.J., Bowring, S.A., 2011. A user's guide to Neoproterozoic geochronology. In: Arnaud, E., Halverson, G.P., Shields-Zhou, G. (Eds.), The Geological Record of Neoproterozoic Glaciations: Geological Society of London, Memoir, 36, pp. 135–149.
Condon, D., Zhu, M.Y., Bowring, S., Wang, W., Yang, A.H., Jin, Y.G., 2005. U—Pb ages from the Neoproterozoic Doushantuo Formation, China. Science 308, 95–98.
Creveling, J.R., Mitrovica, J.X., Chan, N.-H., Latychev, K., Matsuyama, I., 2012. Mechanisms for oscillatory true polar wander. Nature 491, 244–248.
Denyszyn, S.W., Halls, H.C., Davis, D.W., Evans, D.A.D., 2009. Paleomagnetism and U—Pb geochronology of Franklin dykes in High Arctic Canada and Greenland: a revised age and paleomagnetic pole constraining block rotations in the Nares Strait region. Canadian Journal of Earth Sciences 46, 689–705.
Donnadieu, Y., Goddéris, Y., Ramstein, G., Nédelec, A., Meert, J., 2004. A 'snowball Earth' climate triggered by continental break-up through changes in runoff. Nature 428, 303–306.
Dziewonski, A.M., Lekic, V., Romanowicz, B.A., 2010. Mantle anchor structure: an argument for bottom up tectonics. Earth and Planetary Science Letters 299, 69–79.
Ernst, R.E., Wingate, M.T.D., Buchan, K.L., Li, Z.X., 2008. Global record of 1600–700 Ma Large Igneous Provinces (LIPs): implications for the reconstruction of the proposed Nuna (Columbia) and Rodinia supercontinents. Precambrian Research 160, 159–178.
Evans, D.A.D., 2000. Stratigraphic, geochronological, and paleomagnetic constraints upon the Neoproterozoic climatic paradox. American Journal of Science 300, 347–433.
Evans, D.A.D., 2003. A fundamental Precambrian–Phanerozoic shift in Earth's glacial style? Tectonophysics 375, 353–385.
Evans, D.A.D., 2006. Proterozoic low orbital obliquity and axial-dipolar geomagnetic field from evaporite paleolatitudes. Nature 444, 51–55.
Evans, D.A.D., 2010. Proposal with a ring of diamonds. Nature 466, 326–327.
Evans, D.A.D., Raub, T.D., 2011. Neoproterozoic glacial palaeolatitudes: a global update. In: Arnaud, E., Halverson, G.P., Shields-Zhou, G. (Eds.), The Geological Record of Neoproterozoic Glaciations: Geological Society of London, Memoir, 36, pp. 93–112.
Evans, D.A.D., Li, Z.X., Kirschvink, J.L., Wingate, M.T.D., 2000. A high-quality mid-Neoproterozoic paleomagnetic pole from South China, with implications for ice ages and the breakup configuration of Rodinia. Precambrian Research 100, 313–334.
Eyles, N., Januszczak, N., 2004. 'Zipper-rift': a tectonic model for Neoproterozoic glaciations during the breakup of Rodinia after 750 Ma. Earth-Science Reviews 65, 1–73.
Fetter, A.H., Goldberg, S.A., 1995. Age and geochemical characteristics of bimodal magmatism in the Neoproterozoic Grandfather Mountain rift basin. Journal of Geology 103, 313–326.
Frimmel, H.E., Zartman, R.E., Spath, A., 2001. The Richtersveld Igneous Complex, South Africa: U–Pb zircon and geochemical evidence for the beginning of Neoproterozoic continental breakup. Journal of Geology 109, 493–508.
Godderis, Y., Donnadieu, Y., Nédélec, A., Dupré, B., Dessert, C., Grard, A., Ramstein, G., Francois, L.M., 2003. The Sturtian "snowball" glaciation; fire and ice. Earth and Planetary Science Letters 211, 1–12.
Gregory, L.C., Meert, J.G., Bingen, B., Pandit, M.K., Torsvik, T.H., 2009. Paleomagnetism and geochronology of the Malani Igneous Suite, Northwest India: implications for the configuration of Rodinia and the assembly of Gondwana. Precambrian Research 170, 13–26.
Grotzinger, J.P., Fike, D.A., Fischer, W.W., 2011. Enigmatic origin of the largest-known carbon isotope excursion in Earth's history. Nature Geoscience 4, 285–292.
Halverson, G.P., 2006. A Neoproterozoic chronology. In: Xiao, S., Kaufman, A. (Eds.), Neoproterozoic Geobiology and Paleobiology. Vol. 27 of Topics in Geobiology. Springer, Dordrecht, The Netherlands, pp. 231–271.
Halverson, G.P., Shields-Zhou, G., 2011. Chapter 4 Chemostratigraphy and the Neoproterozoic Glaciations. Geological Society, London, Memoirs 36, 51–66.
Halverson, G.P., Hoffman, P.F., Schrag, D.P., Maloof, A.C., Rice, A.H.N., 2005. Toward a Neoproterozoic composite carbon-isotope record. Geological Society of America Bulletin 117, 1181–1207.
Halverson, G.P., Wade, B.P., Hurtgen, M.T., Barovich, K., 2010. Neoproterozoic chemostratigraphy. Precambrian Research 182, 337–350.
Harlan, S.S., Geissman, J.W., Snee, L.W., 1997. Paleomagnetic and $^{40}Ar/^{39}Ar$ geochronologic data from late Proterozoic mafic dykes and sills. Montana and Wyoming: USGS Professional Paper, 1580 (16 pp.).
Harlan, S.S., Heaman, L.M., LeCheminant, A.N., Premo, W.R., 2003. Gunbarrel mafic magmatic event: a key 780 Ma time marker for Rodinia plate reconstructions. Geology 31, 1053–1056.
Hodych, J.P., Cox, R.A., Kosler, J., 2004. An equatorial Laurentia at 550 Ma confirmed by Grenvillian inherited zircons dated by LAM ICP-MS in the Skinner Cove volcanics of

western Newfoundland: implications for inertial interchange true polar wander. Precambrian Research 129, 93–113.
Hoffman, P.F., Grotzinger, J.P., 1993. Orographic precipitation, erosional unloading, and tectonic style. Geology 21, 195–198.
Hoffman, P.F., Li, Z.X., 2009. A palaeogeographic context for Neoproterozoic glaciation. Palaeogeography, Palaeoclimatology, Palaeoecology 277, 158–172.
Hoffman, P.F., Schrag, D.P., 2002. The snowball Earth hypothesis: testing the limits of global change. Terra Nova 14, 129–155.
Hoffman, P.F., Kaufman, A.J., Halverson, G.P., Schrag, D.P., 1998. A Neoproterozoic snowball earth. Science 281, 1342–1346.
Huang, B., Xu, B., Zhang, C., Li, Y., Zhu, R., 2005. Paleomagnetism of the Baiyisi volcanic rocks (ca. 740 Ma) of Tarim, Northwest China: a continental fragment of Neoproterozoic Western Australia? Precambrian Research 142, 83–92.
Hyde, W.T., Crowley, T.J., Baum, S.K., Peltier, W.R., 2000. Neoproterozoic 'snowball Earth' simulations with a coupled climate/ice-sheet model. Nature 405, 425–429.
Ikeda, T., Tajika, E., 1999. A sudy of the energy balance climate model with CO-dependent outgoing radiation: implications for the glaciation during the Cenozoic. Geophysical Research Letters 26, 349–352.
Kah, L.C., Riding, R., 2007. Mesoproterozoic carbon dioxide levels inferred from calcified cyanobacteria. Geology 35, 799–802.
Kirschvink, J.L., 1978. The Precambrian–Cambrian boundary problem: paleomagnetic directions from the Amadeus Basin, central Australia. Earth and Planetary Science Letters 40, 91–100.
Kirschvink, J.L., 1992. Late Proterozoic low-latitude global glaciation: the snowball earth. In: Schopf, J.W., Klein, C. (Eds.), The Proterozoic Biosphere. Cambridge University Press, pp. 51–52.
Kravchinsky, V.A., Konstantinov, K.M., Cogné, J.-P., 2001. Palaeomagnetic study of Vendian and Early Cambrian rocks of South Siberia and Central Mongolia: was the Siberian platform assembled at this time? Precambrian Research 110, 61–92.
Leather, J., Allen, P.A., Brasier, M.D., Cozzi, A., 2002. Neoproterozoic snowball Earth under scrutiny: evidence from the Fiq glaciation of Oman. Geology 30, 891–894.
Levrard, B., Laskar, J., 2003. Climate friction and the Earth's obliquity. Geophysical Journal 154, 970–990.
Li, Z.X., 1998. Tectonic history of the major East Asian lithospheric blocks since the mid-Proterozoic—a synthesis. In: Flower, M.J., Chung, S.-L., Lo, C.-H., Lee, T.-Y. (Eds.), Mantle Dynamics and Plate Interactions in East Asia. Geodynamics Series. American Geophysical Union, Washington, DC, United States, pp. 221–243.
Li, Z.X., Evans, D.A.D., 2011. Late Neoproterozoic 40° intraplate rotation within Australia allows for a tighter-fitting and longer-lasting Rodinia. Geology 39, 39–42.
Li, Z.X., Powell, C.M., 2001. An outline of the palaeogeographic evolution of the Australasian region since the beginning of the Neoproterozoic. Earth-Science Reviews 53, 237–277.
Li, Z.X., Zhong, S., 2009. Supercontinent–superplume coupling, true polar wander and plume mobility: plate dominance in whole-mantle tectonics. Physics of the Earth and Planetary Interiors 176, 143–156.
Li, Z.X., Zhang, L., Powell, C.M., 1995. South China in Rodinia: part of the missing link between Australia–East Antarctica and Laurentia? Geology 23, 407–410.
Li, Z.X., Zhang, L., Powell, C.M., 1996. Positions of the East Asian cratons in the Neoproterozoic supercontinent Rodinia. Australian Journal of Earth Sciences 43, 593–604.
Li, Z.X., Li, X.H., Kinny, P.D., Wang, J., 1999. The breakup of Rodinia: did it start with a mantle plume beneath South China? Earth and Planetary Science Letters 173, 171–181.
Li, Z.X., Li, X.H., Kinny, P.D., Wang, J., Zhang, S., Zhou, H., 2003. Geochronology of Neoproterozoic syn-rift magmatism in the Yangtze Craton, South China and correlations with other continents: evidence for a mantle superplume that broke up Rodinia. Precambrian Research 122, 85–109.
Li, Z.X., Evans, D.A.D., Zhang, S., 2004. A 90° spin on Rodinia: possible causal links between the Neoproterozoic supercontinent, superplume, true polar wander and low-latitude glaciation. Earth and Planetary Science Letters 220, 409–421.
Li, Z.X., Bogdanova, S.V., Collins, A.S., Davidson, A., De Waele, B., Ernst, R.E., Fitzsimons, I.C.W., Fuck, R.A., Gladkochub, D.P., Jacobs, J., Karlstrom, K.E., Lu, S., Natapov, L.M., Pease, V., Pisarevsky, S.A., Thrane, K., Vernikovsky, V., 2008. Assembly, configuration, and break-up history of Rodinia: a synthesis. Precambrian Research 160, 179–210.
Liu, X., Gao, S., Diwu, C., Ling, W., 2008. Precambrian crustal growth of Yangtze Craton as revealed by detrital zircon studies. American Journal of Science 308, 421–468.
Ma, G., Li, H., Zhang, Z., 1984. An investigation of the age limits of the Sinian System in South China. Bulletin of the Yichang Institute of Geology and Mineral Resources, Chinese Academy of Geological Sciences 8, 1–29.
Macdonald, F.A., Schmitz, M.D., Crowley, J.L., Roots, C.F., Jones, D.S., Maloof, A.C., Strauss, J.V., Cohen, P.A., Johnston, D.T., Schrag, D.P., 2010. Calibrating the Cryogenian. Science 327, 1241–1243.
Maloof, A.C., Halverson, G.P., Kirschvink, J.L., Schrag, D.P., Weiss, B.P., Hoffman, P.F., 2006. Combined paleomagnetic, isotopic, and stratigraphic evidence for true polar wander from the Neoproterozoic Akademikerbreen Group, Svalbard, Norway. Geological Society of America Bulletin 118, 1099–1124.
Mbede, E.I., Kampunzu, A.B., Armstrong, R.A., 2004. Neoproterozoic inheritance during Cainozoic rifting in the western and southwestern branches of the East African rift system: evidence from carbonatite and alkaline intrusions. Conference abstract, The East African Rift System: Development, Evolution and Resources, Addis Ababa, Ethiopia, June 20–24, 2004.
McCausland, P.J.A., Hodych, J.P., 1998. Paleomagnetism of the 550 Ma Skinner Cove volcanics of western Newfoundland and the opening of the Iapetus Ocean. Earth and Planetary Science Letters 163, 15–29.
McCausland, P.J.A., Smirnov, A.V., Evans, D., Izard, C., Raub, T.D., 2009. Low-latitude Laurentia at 615 Ma: Paleomagnetism of the Long Range Dykes and Coeval Lighthouse Cove Formation, Northern Newfoundland and SE Labrador. Eos, Transactions of the American Geophysical Union (Abstract GA13B-04).
McCausland, P.J.A., Hankard, F., Van der Voo, R., Hall, C.M., 2011. Ediacaran paleogeography of Laurentia: paleomagnetism and $^{40}Ar—^{39}Ar$ geochronology of the 583 Ma Baie des Moutons syenite, Quebec. Precambrian Research 187, 58–78.
McKenzie, N.R., Hughes, N.C., Myrow, P.M., Choi, D.K., Park, T.-y, 2011. Trilobites and zircons link north China with the eastern Himalaya during the Cambrian. Geology 39, 591–594.
McMechan, M.E., 2000. Neoproterozoic glaciogenic slope deposits, Rocky Mountains, northeast British Columbia. Bulletin of Canadian Petroleum Geology 48, 246–261.
Meert, J.G., Tamrat, E., 2004. A mechanism for explaining rapid continental motion in the Late Neoproterozoic. In: Eriksson, P.G., Altermann, W., Nelson, D.R., Mueller, W.U., Catuneanu, O. (Eds.), The Precambrian Earth: Tempos and Events. Developments in Precambrian Geology, 12. Elsevier, Amsterdam, pp. 255–267.
Meert, J.G., Van der Voo, R., 1996. Paleomagnetic and $^{40}Ar/^{39}Ar$ study of the Sinyai Dolerite, Kenya: implications for Gondwana assembly. Journal of Geology 104, 131–142.
Meert, J.G., Van der Voo, R., Payne, T.W., 1994. Paleomagnetism of the Catoctin Volcanic Province—a New Vendian–Cambrian apparent polar wander path for North-America. Journal of Geophysical Research-Solid Earth 99, 4625–4641.
Meert, J.G., Van der Voo, R., Ayub, S., 1995. Paleomagnetic investigation of the Late Proterozoic Gagwe lavas and Mbozi complex, Tanzania and the assembly of Gondwana. Precambrian Research 74, 225–244.
Metelkin, D.V., Belonosov, I.V., Gladkochub, D.P., Donskaya, T.V., Mazukabzov, A.M., Stanevich, A.M., 2005. Paleomagnetic directions from Nersa intrusions of the Biryusa terrane, Siberian Craton, as a reflection of tectonic events in the Neoproterozoic. Russian Geology and Geophysics 46, 398–413.
Miller, K.C., Hargraves, R.B., 1994. Paleomagnetism of Some Indian Kimberlites and Lamproites. Precambrian Research 69, 259–267.
Miller, K.G., Kominz, M.A., Browning, J.V., Wright, J.D., Mountain, G.S., Katz, M.E., Sugarman, P.J., Cramer, B.S., Christie-Blick, N., Pekar, S.F., 2005. The Phanerozoic record of global sea-level change. Science 310, 1293–1298.
Mitchell, R.N., Kilian, T.M., Raub, T.D., Evans, D.A.D., Bleeker, W., Maloof, A.C., 2011. Sutton hotspot track: resolving Ediacaran–Cambrian tectonics and true polar wander of Laurentia. American Journal of Science 311, 651–663.
Mitchell, R.N., Kilian, T.M., Evans, D.A.D., 2012. Supercontinent cycles and the calculation of absolute palaeolongitude in deep time. Nature 482, 208–211.
Moloto-A-Kenguemba, G.R., Trindade, R.I.F., Monié, P., Nédélec, A., Siqueira, R., 2008. A late Neoproterozoic paleomagnetic pole for the Congo craton: tectonic setting, paleomagnetism and geochronology of the Nola dike swarm (Central African Republic). Precambrian Research 164, 214–226.
Morel, P., 1981. Palaeomagnetism of a Pan-African diorite: a Late Precambrian pole for western Africa. Geophysical Journal of the Royal Astronomical Society 65, 493–503.
Muller, R.D., Sdrolias, M., Gaina, C., Steinberger, B., Heine, C., 2008. Long-term sea-level fluctuations driven by ocean basin dynamics. Science 319, 1357–1362.
Murthy, G.S., 1971. The paleomagnetism of diabase dikes from the Grenville Province. Canadian Journal of Earth Sciences 8, 802–812.
Myrow, P.M., Hughes, N.C., Goodge, J.W., Fanning, C.M., Williams, I.S., Peng, S.C., Bhargava, O.N., Parcha, S.K., Pogue, K.R., 2010. Extraordinary transport and mixing of sediment across Himalayan central Gondwana during the Cambrian–Ordovician. Geological Society of America Bulletin 122, 1660–1670.
Park, J.K., Norris, D.K., Larochelle, A., 1989. Paleomagnetism and the origin of the Mackenzie Arc of northwestern Canada. Canadian Journal of Earth Sciences 26, 2194–2203.
Pierrehumbert, R.T., 2004. High levels of atmospheric carbon dioxide necessary for the termination of global glaciation. Nature 429, 646–649.
Pisarevsky, S.A., Gurevich, E.L., Khramov, A.N., 1997. Palaeomagnetism of Lower Cambrian sediments from the Olenek River section (northern Siberia): palaeopoles and the problem of magnetic polarity in the Early Cambrian. Geophysical Journal International 130, 746–756.
Pisarevsky, S.A., Komissarova, R.A., Khramov, A.N., 2000. New palaeomagnetic result from Vendian red sediments in Cisbaikalia and the problem of the relationship of Siberia and Laurentia in the Vendian. Geophysical Journal International 140, 598–610.
Pisarevsky, S.A., Wingate, M.T.D., Stevens, M.K., Haines, P.W., 2007. Palaeomagnetic results from the Lancer 1 stratigraphic drillhole, Officer Basin, Western Australia, and implications for Rodinia reconstructions. Australian Journal of Earth Sciences 54, 561–572.
Pisarevsky, S.A., Murphy, J.B., Cawood, P.A., Collins, A.S., 2008. Late Neoproterozoic and Early Cambrian palaeogeography: models and problems. In: Pankhurst, R.J., Trouw, R.A.J., Brito Neves, B.B., de Wit, M.J. (Eds.), West Gondwana: Pre-Cenozoic Correlations Across the South Atlantic Region: Geological Society, London, Special Publications, 294, pp. 9–31.
Popov, V., Iosifidi, A., Khramov, A., Tait, J., Bachtadse, V., 2002. Paleomagnetism of Upper Vendian sediments from the Winter Coast, White Sea region, Russia: implications for the paleogeography of Baltica during Neoproterozoic times. Journal of Geophysical Research 107 (B11). http://dx.doi.org/10.1029/2001JB001607.
Powell, C.M., Preiss, W.V., Gatehouse, C.G., Krapez, B., Li, Z.X., 1994. South Australian record of a Rodinian epicontinental basin and its mid-Neoproterozoic breakup (~700 Ma) to form the palaeo-Pacific Ocean. Tectonophysics 237, 113–140.
Rainbird, R.H., Ernst, R.E., 2001. The sedimentary record of mantule–plume uplift. In: Ernst, R.E., Buchan, K.L. (Eds.), Mantle Plumes: Their Identification Through Time: Geological Society of America Special Paper, 352, pp. 227–245.
Rainbird, R.H., Jefferson, C.W., Young, G.M., 1996. The early Neoproterozoic sedimentary Succession B of northwestern Laurentia: correlations and paleogeographic significance. Geological Society of America Bulletin 108, 454–470.

Rooney, A., Macdonald, F., 2012. Neoproterozoic glaciations and post-glacial weathering regimes: insights from Re—Os geochronology and Os isotope stratigraphy. Fermor Meeting 2012, The Neoproterozoic Era: Evolution, Glaciation and Oxygenation, London.
Russell, K.L., 1968. Oceanic ridges and eustatic changes in sea level. Nature 218, 861–862.
Sánchez-Bettucci, L., Rapalini, A.E., 2002. Paleomagnetism of the Sierra de Las Animas Complex, southern Uruguay: its implications in the assembly of western Gondwana. Precambrian Research 118, 243–265.
Schmidt, P.W., Williams, G.E., 1996. Palaeomagnetism of the ejecta-bearing Bunyeroo Formation, late Neoproterozoic, Adelaide fold belt, and the age of the Acraman impact. Earth and Planetary Science Letters 144, 347–357.
Schmidt, P.W., Williams, G.E., 2010. Ediacaran palaeomagnetism and apparent polar wander path for Australia: no large true polar wander. Geophysical Journal International 182, 711–726.
Schmidt, P.W., Williams, G.E., McWilliams, M.O., 2009. Palaeomagnetism and magnetic anisotropy of late Neoproterozoic strata, South Australia: implications for the palaeolatitude of late Cryogenian glaciation, cap carbonate and the Ediacaran System. Precambrian Research 174, 35–52.
Schrag, D.P., Berner, R.A., Hoffman, P.F., Halverson, G.P., 2002. On the initiation of a snowball Earth. Geochemistry, Geophysics, Geosystems 3. http://dx.doi.org/10.1029/2001GC000219.
Sohl, L.E., Christie-Blick, N., Kent, D.V., 1999. Paleomagnetic polarity reversals in Marinoan (ca. 600 Ma) glacial deposits of Australia: implications for the duration of low-latitude glaciation in Neoproterozoic time. Geological Society of America Bulletin 111, 1120–1139.
Squire, R.J., Campbell, I.H., Allen, C.M., Wilson, C.J.L., 2006. Did the Transgondwanan Supermountain trigger the explosive radiation of animals on Earth? Earth and Planetary Science Letters 250, 116–133.
Stern, R.J., Johnson, P., 2010. Continental lithosphere of the Arabian Plate: a geologic, petrologic, and geophysical synthesis. Earth-Science Reviews 101, 29–67.
Swanson-Hysell, N.L., Maloof, A.C., Kirschvink, J.L., Evans, D.A.D., Halverson, G.P., Hurtgen, M.T., 2012. Constraints on Neoproterozoic paleogeography and Paleozoic orogenesis from paleomagnetic records of the Bitter Springs Formation, Amadeus Basin, central Australia. American Journal of Science 312, 817–884.
Symons, D.T.A., Chiasson, A.D., 1991. Paleomagnetism of the Callander Complex and the Cambrian apparent polar wander path for North America. Canadian Journal of Earth Sciences 28, 355–363.
Tanczyk, E.I., Lapointe, P., Morris, W.A., Schmidt, P.W., 1987. A paleomagnetic study of the layered mafic intrusion at Sept-Îles, Quebec. Canadian Journal of Earth Sciences 24, 1431–1438.
Torsvik, T.H., Muller, R.D., Van der Voo, R., Steinberger, B., Gaina, C., 2008. Global plate motion frames: toward a unified model. Reviews of Geophysics 46 (3), RG3004. http://dx.doi.org/10.1029/2007RG000227.
Torsvik, T.H., Burke, K., Steinberger, B., Webb, S.J., Ashwal, L.D., 2010. Diamonds sampled by plumes from the core–mantle boundary. Nature 466, 352–355.
Trindade, R.I.F., Font, E., D'Agrella-Filho, M.S., Nogueira, A.C.R., Riccomini, C., 2003. Low-latitude and multiple geomagnetic reversals in the Neoproterozoic Puga cap carbonate, Amazon craton. Terra Nova 15, 441–446.
Valentine, J.W., Moores, E.M., 1970. Plate-tectonic regulation of faunal diversity and sea level: a model. Nature 228, 657–659.
Veevers, J.J., Belousova, E.A., Saeed, A., Sircombe, K., Cooper, A.F., Read, S.E., 2006. Pan-Gondwanaland detrital zircons from Australia analysed for Hf-isotopes and trace elements reflect an ice-covered Antarctic provenance of 700–500 Ma age, TDM of 2.0–1.0 Ga, and alkaline affinity. Earth-Science Reviews 76, 135–174.
Voigt, A., Abbo, D.S., 2012. Sea-ice dynamics strongly promote Snowball Earth initiation and destabilize tropical sea-ice margins. Climate of the Past Discussions 8, 2079–2092.
Walderhaug, H.J., Torsvik, T.H., Eide, E.A., Sundvoll, B., Bingen, B., 1999. Geochronology and palaeomagnetism of the Hunnedalen dykes, SW Norway: implications for the Sveconorwegian apparent polar wander loop. Earth and Planetary Science Letters 169, 71–83.
Walderhaug, H.J., Torsvik, T.H., Halverson, E., 2007. The Egersund dykes (SW Norway): a robust Early Ediacaran (Vendian) palaeomagnetic pole from Baltica. Geophysical Journal International 168, 935–948.
Wang, J., Li, Z.X., 2003. History of Neoproterozoic rift basins in South China: implications for Rodinia break-up. Precambrian Research 122, 141–158.
Wang, X.C., Li, X.H., Li, W.X., Li, Z.X., 2007. Ca. 825 Ma komatiitic basalts in South China: First evidence for > 1500 degrees C mantle melts by a Rodinian mantle plume. Geology 35, 1103–1106.
Wang, X.C., Li, X.H., Li, Z.X., Liu, Y., Yang, Y.H., 2010. The Willouran basic province of South Australia: its relation to the Guibei large igneous province in South China and the breakup of Rodinia. Lithos 119, 569–584.
Wang, X.C., Li, Z.X., Li, X.H., Li, Q.L., Zhang, Q.R., 2011. Geochemical and Hf—Nd isotope data of Nanhua rift sedimentary and volcaniclastic rocks indicate a Neoproterozoic continental flood basalt provenance. Lithos 127, 427–440.
Weil, A.B., Geissman, J.W., Van der Voo, R., 2004. Paleomagnetism of the Neoproterozoic Chuar Group, Grand Canyon Supergroup, Arizona: implications for Laurentia's Neoproterozoic APWP and Rodinia break-up. Precambrian Research 129, 71–92.
Williams, G.E., Schmidt, P.W., 2004. Neoproterozoic glaciation: reconciling low paleolatitudes and the geologic record. In: Jenkins, G.S., McMenamin, M., Sohl, L.E., McKay, C.P. (Eds.), The Extreme Proterozoic: Geology, Geochemistry and Climate. Geophysical Monograph American Geophysical Union, Washington, pp. 145–159.
Williams, S.E., Müller, R.D., Landgrebe, T.C., Whittaker, J.M., 2012. An open-source software environment for visualizing and refining plate tectonic reconstructions using high-resolution geological and geophysical data sets. GSA Today 22 (4/5), 4–9.
Wingate, M.T.D., Giddings, J.W., 2000. Age and palaeomagnetism of the Mundine Well dyke swarm, Western Australia: implications for an Australia–Laurentia connection at 755 Ma. Precambrian Research 100, 335–357.
Wingate, M.T.D., Campbell, I.H., Compston, W., Gibson, G.M., 1998. Ion microprobe U—Pb ages for Neoproterozoic basaltic magmatism in south-central Australia and implications for the breakup of Rodinia. Precambrian Research 87, 135–159.
Wingate, M.T.D., Pisarevsky, S.A., De Waele, B., 2010. Paleomagnetism of the 765 Ma Luakela Volcanics in northwest Zambia and implications for Neoproterozoic positions of the Congo craton. American Journal of Science 310, 1333–1344.
Xu, B., Xiao, S., Zou, H., Chen, Y., Li, Z.-X., Song, B., Liu, D., Zhou, C., Yuan, X., 2009. SHRIMP zircon U—Pb age constraints on Neoproterozoic Quruqtagh diamictites in NW China. Precambrian Research 168, 247–258.
Yao, W.H., Li, Z.X., Li, W.X., Li, X.H., Yang, J.H., 2013w. From Rodinia to Gondwanaland: a tale from detrital provenance analyses of the Cathaysia Block, South China (under review).
Zhan, S., Chen, Y., Xu, B., Wang, B., Faure, M., 2007. Late Neoproterozoic paleomagnetic results from the Sugetbrak Formation of the Aksu area, Tarim basin (NW China) and their implications to paleogeographic reconstructions and the snowball Earth hypothesis. Precambrian Research 154, 143–158.
Zhang, S., Li, Z.X., Wu, H., 2006. New Precambrian palaeomagnetic constraints on the position of the North China Block in Rodinia. Precambrian Research 144, 213–238.
Zhang, S., Li, Z.X., Evans, D.A.D., Wu, H., Li, H., Dong, J., 2012. Pre-Rodinia supercontinent Nuna shaping up: a global synthesis with new paleomagnetic results from North China. Earth and Planetary Science Letters 353–354, 145–155.
Zhang, S., Evans, D.A.D., Li, H., Wu, H., Jiang, G., Dong, J., Zhao, Q., Raub, T., Yang, T., 2013. Paleomagnetism of the late Cryogenian Nantuo Formation and paleogeographic implications for the South China Block. Journal of Asian Earth Sciences 72, 164–177.